



Delft University of Technology

Advancing railway track health monitoring Integrating GPR, InSAR and machine learning for enhanced asset management

Koohmishi, Mehdi; Kaewunruen, Sakdirat; Chang, Ling; Guo, Yunlong

DOI

[10.1016/j.autcon.2024.105378](https://doi.org/10.1016/j.autcon.2024.105378)

Publication date

2024

Document Version

Final published version

Published in

Automation in Construction

Citation (APA)

Koohmishi, M., Kaewunruen, S., Chang, L., & Guo, Y. (2024). Advancing railway track health monitoring: Integrating GPR, InSAR and machine learning for enhanced asset management. *Automation in Construction*, 162, Article 105378. <https://doi.org/10.1016/j.autcon.2024.105378>

Important note

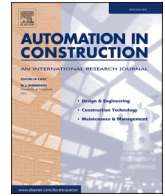
To cite this publication, please use the final published version (if applicable).
Please check the document version above.

Copyright

Other than for strictly personal use, it is not permitted to download, forward or distribute the text or part of it, without the consent of the author(s) and/or copyright holder(s), unless the work is under an open content license such as Creative Commons.

Takedown policy

Please contact us and provide details if you believe this document breaches copyrights.
We will remove access to the work immediately and investigate your claim.



Review

Advancing railway track health monitoring: Integrating GPR, InSAR and machine learning for enhanced asset management

Mehdi Koohmishi^a, Sakdirat Kaewunruen^b, Ling Chang^c, Yunlong Guo^{d,*}

^a Department of Civil Engineering, Faculty of Engineering, University of Bojnord, Bojnord, Iran

^b Department of Civil Engineering, School of Engineering, University of Birmingham, Birmingham B152TT, United Kingdom

^c Faculty of Geo-Information Science and Earth Observation (ITC), University of Twente, 7514AE Enschede, the Netherlands

^d Faculty of Civil Engineering and Geosciences, Delft University of Technology, Delft 2628CN, Netherlands

ARTICLE INFO

Keywords:

Railway ballasted track
SAR interferometry
InSAR
Ground-penetrating radar
GPR
Non-destructive testing
Machine learning
Inspection
Condition-based railway maintenance

ABSTRACT

Railway track health monitoring and maintenance are crucial stages in railway asset management, aiming to enhance the train operation quality and service life. For this aim, various inspection means (using diverse non-destructive testing techniques) have been applied, however, these means are mostly not able to monitor whole railway track network or track underlying layers (e.g., ballast and subgrade). The use of remote sensing techniques, such as Interferometric Synthetic Aperture Radar (InSAR), can expedite the defect diagnosis process for railway tracks, elevating the scope of health monitoring to a network-wide level. The Ground Penetrating Radar (GPR) has emerged as a particularly reliable method, especially for detecting structural deficiencies in underlying layers. As a result, combining the two distinct non-destructive testing techniques – GPR and InSAR – presents a promising strategy for efficient railway asset management. Recognizing the significance of embracing newer and more advanced monitoring strategies, this paper reviews the fusion of GPR and InSAR methodologies, and explores the potential integration of machine learning models to develop a predictive health monitoring and condition-based maintenance approach for railway tracks.

1. Introduction

1.1. Background

Although there has been a surge in the development of slab railway tracks in recent decades, ballasted tracks remain the predominant structure for railway lines globally. As shown in Fig. 1, the structural components of ballasted tracks comprise sleepers, fastening systems, and rails, which are categorized as the superstructure. The granular media, such as ballast, sub-ballast, subgrade and embankment, are considered part of the substructure. Depending on the perspective, the ballast layer is classified either as a component of the superstructure [1,2] or the substructure [3,4]. The combined effects of higher speeds and increased axle loads necessitate expanded maintenance activities, especially stemming from the rapid degradation of the railway granular media.

Fig. 2 illustrates that the life span of a railway track can be segmented into three distinct periods: youth, intermediate-life, and old-age [6]. With this understanding, emphasizing predictive and condition-

based maintenance approaches emerge as more efficient strategy for cost-effective smart railway maintenance. Statistically, the average annual maintenance and renewal (M&R) expenses per 1 km of tracks amount to approximately €50,000 for West-European networks [7,8]. Consequently, adopting a predictive and condition-based maintenance is more effective than corrective maintenance [9]. Leveraging non-destructive testing (NDT) techniques for railway track health monitoring proves to be a more valuable maintenance strategy.

To archive the goal of smart maintenance, firstly the criteria for track quality assessment are introduced as follows. Track geometry is the most widely-used criterion, which involves alignment, longitudinal level, twisting, etc. (mostly related to track accumulated deformation) [10,11]. Another criterion is train-track dynamic responses (mostly related to track stiffness). Vibration-based techniques can quantify track stiffness [12], while optical-based/remote sensing methods are able to diagnose deformation [13]. Numerous non-destructive testing techniques (NDTs) are employed to inspect track components, which can be categorized into optical-based tools, inertial methods, acoustic and ultrasonic techniques, and imaging-based analyses. These NDT techniques

* Corresponding author.

E-mail address: yunlong.guo@tudelft.nl (Y. Guo).

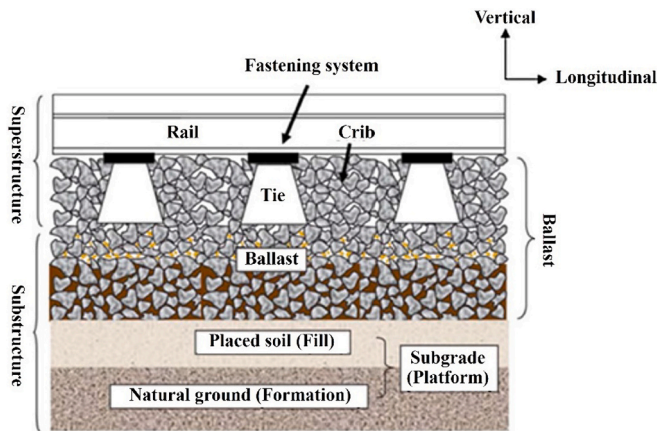


Fig. 1. Components of conventional railway ballasted track [3,5].

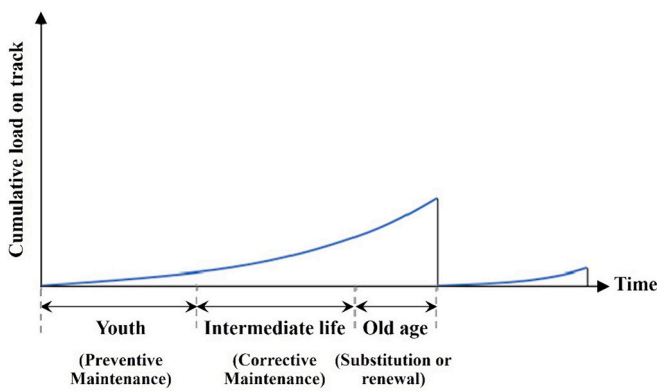


Fig. 2. Process of deterioration of ballasted railway tracks - Characterizing the corresponding maintenance actions based on the correspondent time [6].

will be introduced briefly, while GPR and InSAR will be stressed, as well as applications of their combination.

Among railway granular materials, ballast is the most vulnerable component and key component for track geometry correction. Its service life is intricately linked to maintenance activities and track usage. For German ballasted railway tracks, reference [6] indicates that the typical life cycles for ballast tamping, cleaning, and renewal are 4–5, 12–15, and 20–30 years, respectively. However, in China, due to more frequent tamping and stabilization, combined with the effects of heavily operated trains and heavy haul, the service life of ballast is nearly halved in comparison to these values [14]. Given the life cycle costs associated with ballast, it becomes imperative to optimize ballast tamping and renewal [15]. Moreover, the cumulative deformation arising from ballast degradation expedites the deterioration of other components, such as rail fractures, ballast pockets, and fastener failures. Consequently, for reasons of safety and ride comfort, the primary challenge in smart railway maintenance lies in avoiding excessive and frequent maintenance and renewal activities. Furthermore, shifting the focus towards a predictive maintenance approach, rather than simply reacting to faults or persistently regular maintenance, is becoming the preferred strategy for managing railway track rehabilitation and maintenance.

1.2. Railway track deterioration: a focus on track geometry and degradation of ballast/sub-ballast layers and subgrade

Overall, various defects can manifest in different components of railway ballasted tracks. The substructure, in particular, plays a critical role in the emergence of these deteriorations. Specifically, the vertical and lateral deformations of granular media, as well as the degradation of

ballast particles, are primary defects associated with these underlying components. The ballast deformation process comprises two stages: initial consolidation post-renewal or tamping, followed by degradation of the ballast aggregates leading to further densification [16,17]. Moreover, certain fouling materials in the ballast, like coal dust, can act as lubricants, exacerbating permanent deformation in this granular layer [18]. Ultimately, these internal and external sources of fouling result in poorly-draining ballast, accelerating track deterioration. Box test results on both dry and saturated specimens of abraded ballast fouled with windblown particles have confirmed increased settlement [19].

Regarding the other substructure components, common failure modes for the subgrade and embankments of railway tracks include settlement, shear failure, and erosion [20]. Depending on the characteristics of the underlying soil layers, loess subgrades with large-sized pores might experience significant settlement [21]. Similarly, silt subgrades under train loading with escalating speeds might also lead to sharp increases in cumulative deformation [22]. Additionally, groundwater drawdown is identified as a significant factor that contributes to the residual settlement observed during dry seasons [23].

There exists a direct correlation between the condition of the ballast layer/track component defects and the track geometry irregularities of railway lines [10,24]. For example, Nabochenko et al. [25] identified the deterioration of railway track geometry resulting from uneven subsidence of the ballast layer. Wang et al. [26] sought to understand the relationship between track geometry defects and substructure conditions. They integrated data from a passenger railway that covered geometry defects, substructure conditions, maintenance history, as well as curvature and turnout information. Their establishment of data-driven models validated that surfacing activities, such as tamping and ballast renewal, were the predominant factors influencing the predicted occurrence of geometry defects. In summary, ballast/subgrade degradation, ballast fouling, poor track drainage conditions, and sub-optimal monitoring/maintenance are the primary contributors to rapid track deterioration.

1.3. Defect diagnosis and maintenance implementation

Based on system reliability, a significant portion of maintenance costs for railway infrastructures is allocated towards improving geometrical characteristics [27]. Furthermore, the desired reliability level profoundly impacts the maintenance budget. As noted by Bressi et al. [8], an increase in the reliability level from 75% to 85% necessitates a 22% boost in the budget allocated to railway track maintenance. In contrast, raising the reliability from 85% to 95% requires a budget increase of 114%. Burkhalter and Adey [28] delved further into establishing an optimized strategy for railway asset interventions, ensuring the best measures are taken for selected infrastructure at the optimal time. Given that track geometry (TG) monitoring serves as an effective method to assess track structural conditions, an interactive fuzzy linear assignment method (IFLAM) has been introduced to choose the ideal maintenance strategy for railway infrastructures [29]. Therefore, it is vital to prioritize the detection of defects through continuous railway track monitoring, setting the stage for timely maintenance actions.

In this context, to assess conditions of the ballast layer by employment of stand-alone technologies, including fouling levels and moisture content, utilizing ground penetrating radar (GPR) emerges as a fitting non-destructive method [30]. In addition, employing imaging-based methods is invaluable for inspecting the condition of the land on which the railway is constructed. For instance, interferometric synthetic aperture radar (InSAR) offers a rapid means of diagnosing track settlement (or subsidence) in whole railway networks.

Though stand-alone NDTs have been widely extended, integration of different technologies can be characterized as a practical approach to solve gaps emerging from singular technology. Moreover, data fusion of different methods/equipment/scale domains/precisions is gaining further momentum nowadays upon which more sophisticated models

can be developed [31,32]. Generally, various data-integration procedures are available to integrate information collected through distinct NDT methods, such as geostatistical analysis [33], employment of datasets of different spatial and temporal resolutions [34], as well as downscaling/upscaling data derived by remote sensing [35]. In addition, integrating data from NDT inspections as input for building information modelling (BIM) is practical to create a unified environment for linear transport infrastructure [36,37]. Regarding current study, synergistic combination of InSAR and GPR techniques provides multi-scale exchange of information.

To illustrate the stand-alone employment of InSAR and GPR techniques for railway monitoring, alongside the data fusion of InSAR and GPR, a literature review was conducted on Scopus scientific database from 2008 to 2023 [38]. Fig. 3 represents the number of publications as well as the citation count of selected papers with respect to characterized keywords.

1.4. Aim and objectives

To evaluate the viability of merging different NDTs, this paper explores the combined use of InSAR and GPR techniques to enhance the health monitoring process for railway infrastructures, with a particular emphasis on railway tracks. Additionally, this paper delves into the potential integration of machine learning models in asset management to determine the feasibility of a predictive and condition-based maintenance. The structure of this review paper encompasses the following

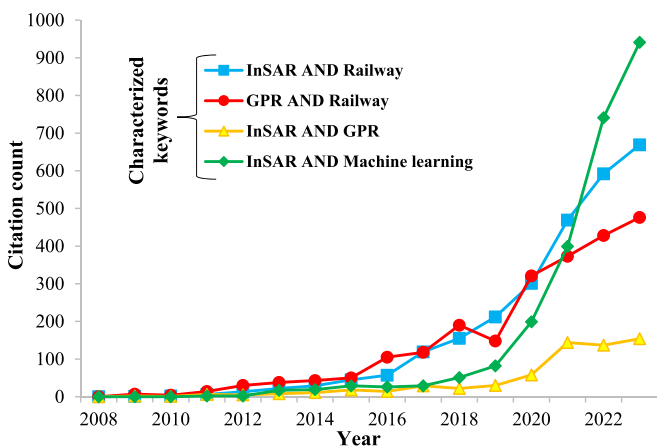
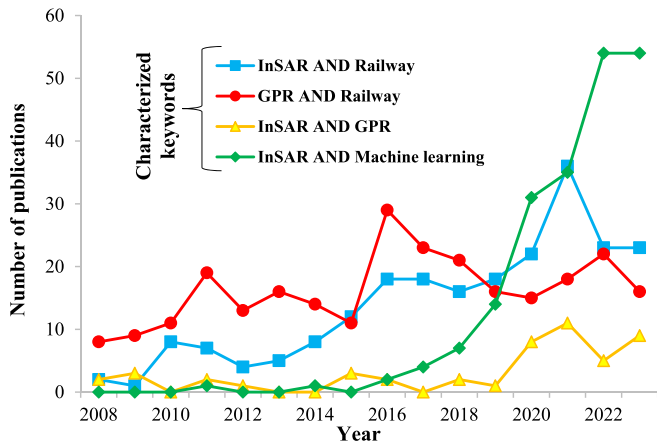


Fig. 3. Statistical analysis of relevant literature based on Scopus scientific database from 2008 to 2023 [38].

sections:

- Destructive vs. non-destructive methods for the health monitoring of railway ballasted tracks;
- A concise overview of InSAR and GPR techniques;
- Independent application of specific NDT techniques for evaluating infrastructures, with a primary focus on railway tracks;
- Combined integration of InSAR and GPR to merge NDTs for enhanced health monitoring of infrastructures, emphasizing railway tracks;
- Adoption of ML methods in specified health monitoring techniques, specifically InSAR and GPR, to formulate predictive and condition-based maintenance strategies.

Fig. 4 provides a visual representation of the research gaps identified in prior studies and the primary contributions of this review article.

2. Methods for health monitoring of tracks

2.1. Destructive methods

Aside from NDTs, traditional destructive methods for monitoring railway tracks have maintained significant relevance. Specifically, excavating holes to retrieve samples for sieving remains a conventional technique, though it is occasionally used to validate GPR results. For instance, in Nebraska, in-service field ballast was sieved to analyse particle size distribution changes alongside particle morphological properties [39].

For GPR result validation, several field studies have been undertaken to validate the GPR capability in estimating the thickness of granular layers, fouling levels, and drainage conditions. These studies either involve constructing trial embankments with varying materials, moisture contents, and thicknesses or involve digging trenches [5,40–43]. For example, Kashani et al. [42] conducted a comprehensive laboratory test to establish the relationship between fouled ballast and GPR data, considering three fouling percentages by reconfiguring the physical model three times. Artagan and Borecky [43] explored the feasibility of using GPR with different frequencies to evaluate the condition of railway granite ballast by excavating trenches in crib ballast situated on the track axis and shoulder.

Both destructive and non-destructive measurements have confirmed that an increase in fouling levels leads to a rise in relative dielectric permittivity. In terms of relevant intrusive techniques, Mishra et al. [44,45] employed a multi-depth deflectometer to examine differential movements of three railway bridge approaches, using sensors installed at layer interfaces via small-diameter holes. Haddani et al. [46] combined the use of PANDA and geo-endoscopy to enhance M&R plan processes. The former assessed the mechanical properties of ballast layer in-depth, based on cone resistance evolution, while the latter determined the thickness and gradation of layers from videos recorded by an endoscopic probe inserted into the hole. As highlighted by Vivanco et al. [47], these tests were integrated, named Pandoscope, to ascertain the level of ballast fouling.

2.2. Non-destructive testing methods

Various methods employing NDT techniques have been developed to monitor the health conditions of railway tracks. For instance, Papaalias et al. [48] compiled a list of viable NDTs that can detect rail defects. Similarly, Ferrante et al. [49] categorized existing NDTs based on the productivity of the approach and the resolution of the results. Table 1 provides a summary of NDT methods (from earlier research and review articles) used for assessing the health condition of ballasted railway tracks.

Given the aforementioned NDT methods, InSAR stands out for global productive inspection due to its ability to collect data under various

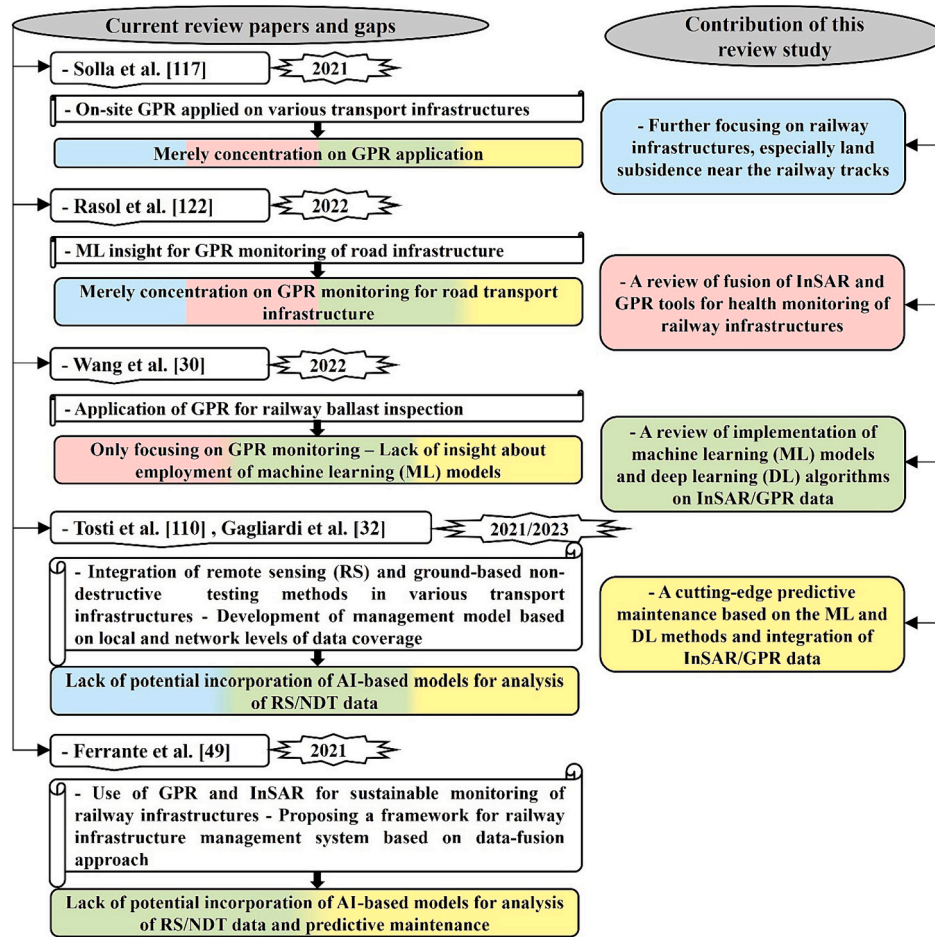


Fig. 4. Illustrative layout of the framework and contribution of this review study.

weather conditions, its wide coverage area (potential in railway network scale), and the repeatability of observations. GPR is also a well-established NDT that minimally interferes with local traffic and is highly effective in surveying the interiors of the ballast layer, subgrade, and embankment. In the subsequent sections of this review paper, we delve deeper into the background of InSAR and GPR techniques. We also explore the use of these remote sensing and ground-based NDT techniques for structural health monitoring across various transport infrastructures.

2.2.1. InSAR

SAR, a subset of satellite remote sensing tools, leverages space technology to continuously monitor ground deformation around infrastructures, such as railway tracks. The amplitude and phase are the primary components of SAR imagery data, measured based on the emitted and received signals of electromagnetic waves. To discern changes in land surface topography, the temporal phase variations captured by sensors over time are harnessed by utilizing a potent feature known as SAR interferometry (InSAR). Indeed, deformation values are captured through corresponding data acquisition times, resulting in the creation of an interferogram and deformation map [67,68]. The ability of this technique to penetrate clouds makes it highly versatile for various conditions, from clear to adverse weather and from daytime to nighttime, with regular data updates and global coverage (as depicted in Fig. 5). The interferometric phase represents the phase difference between two SAR acquisitions, which is vital for determining surface displacement and encompasses the following components [32,65,69,70]:

$$\Delta\varphi = \Delta\varphi_{\text{topo}} + \Delta\varphi_{\text{def}} + \Delta\varphi_{\text{atm}} + \Delta\varphi_{\text{noise}} - 2\pi a \quad (1)$$

$\Delta\varphi$ = Total observed interferometric phase, confined in $[-\pi, \pi]$.

$\Delta\varphi_{\text{topo}}$ = Topographic phase.

$\Delta\varphi_{\text{def}}$ = Displacement phase representing the surface deformation.

$\Delta\varphi_{\text{atm}}$ = Atmospheric phase component.

$\Delta\varphi_{\text{noise}}$ = Unmodeled noise phase component.

a = Phase ambiguity number.

After phase unwrapping, the displacement [in meters] in the slant range direction can be calculated by [32]:

$$\Delta R = \frac{\lambda}{4\pi} \Delta\varphi_{\text{def}} \quad (2)$$

ΔR = Displacement in the slant range direction (m).

λ = Radar wavelength.

The prevailing methods extended for analysis of SAR images are permanent scatterers InSAR (PS-InSAR) and small baseline subset (SBAS) InSAR. Regarding the first technique, a point-based outcome is generated by exploiting multiple SAR images, while one image is characterized as single master. Considering SBAS InSAR, a network of image pairs is generated by restricting temporal and spatial baselines [73,74].

2.2.2. GPR

GPR is an electromagnetic-based device designed for inspecting the subsurface conditions of various infrastructures, such as the ballast layer, subgrade layers and embankment of railway tracks. Sussmann et al. [75] emphasized the analysis of GPR data to recognize changes in reflection intensity and the time of maximum reflection intensity. These changes facilitate the identification of both thickness and variations in

Table 1
Classification of non-destructive methods for health monitoring of ballasted tracks - Laboratory scale, railway line scale, railway network scale.

Reference	Established methods	System applied	Defects detected/Monitoring applied	Monitoring scale
Liu et al. [50]	Vibration-based method	Using a test box filled with ballast, applying impact hammer test	Measuring vibration characteristics, such as time-domain curve of acceleration	Laboratory scale
Haji Abdulrazzagh et al. [51]		Determination of deflection basin based on the applied impact load via falling weight deflectometer (FWD)	Employment of back-analysis techniques to derive the ballast and subgrade moduli	Railway line scale
Moaveni et al. [52], Huang et al. [53]	Visual inspection alongside image processing algorithms	Using digital single-lens reflex (DSLR) camera as well as collecting ballast samples from mainline freight railways	Analysis of size and shape properties of aggregate particles	Laboratory scale
Schmidt et al. [54]		Combing the results of permeability tests and data acquisition based on the image processing method	Determining the appropriate time for interfering and implementing the ballast cleaning	Laboratory scale
Guerrieri et al. [55]		Employment of DIP	Detection of rail corrugation and ballast gradation	Laboratory scale
Hussaini et al. [56], Sasi et al. [57]	Optic-based method	Using fibre optic sensors (FOS)	Ballast lateral displacement and localized strain	Laboratory scale
Benedetto et al. [58]	Electromagnetic, such as Ground penetration radar (GPR)	GPR device with frequencies of 1 GHz and 2 GHz	Relationship between ballast fouling and GPR results	Laboratory scale
Bianchini Ciampoli et al. [59,60]		GPR device with frequencies of 1 GHz and 2 GHz	Detecting the fouling and fragmentation of ballast, and figuring out evident efficacy of fouling rate on electromagnetic response under wet conditions	30 m-long railway line scale
Aldao et al. [61]	Light detection and ranging (LiDAR)	Using solid-state LiDAR system mounted on a mobile trolley	Measuring displacement of a ballast layer and derivation of a digital elevation model	Railway line scale
Liang et al. [62]	Infrared Thermography	Using infrared thermal imager for detecting infrared radiation energy and producing thermograms	Detecting the fouling level of ballast based on the temperature differences	Railway line scale
Narazaki et al. [63]	UAV/Drones	Unmanned aerial vehicles	Flexible observation platforms and covering inaccessible areas	Railway line scale
Singh et al. [64]			Computing gauge measurement	Railway line scale
Poreh et al. [65]	Satellite remote sensing, such as InSAR	Using 25 X-band radar images of Cosmo-SkyMed (CSK)	Evaluation of deformation rate	A particular railway bridge
Wassie et al. [66]		Using Sentinel-1 A/B images	Monitoring land subsidence along railway infrastructures	a 60-km railway line

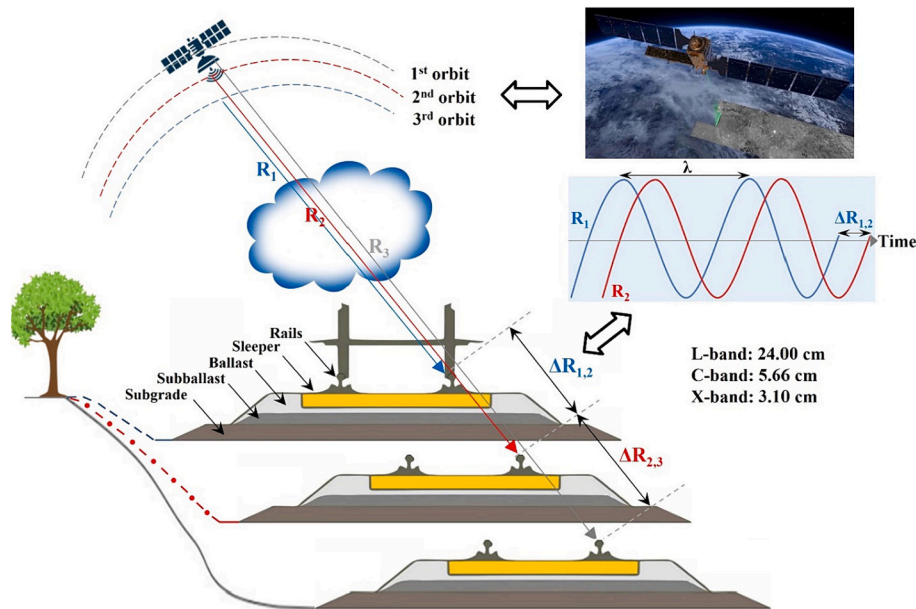


Fig. 5. Schematic layout of extraction of land surface displacement near the railway track by InSAR technique [adapted from Ferrante et al. [49], D'Amico et al. [71], Gagliardi et al. [72]].

the dielectric constant. Roberts et al. [76] noted that using GPR to assess the subsurface of a railway track is feasible. To determine the properties of materials within the substructure of the railway track, the dielectric permittivity is calculated using the following equations [41,60]:

$$\epsilon_r = \left(\frac{c}{v}\right)^2 \quad (3)$$

ϵ_r = Dielectric permittivity.

c = Velocity of propagation of electromagnetic waves through the air (3×10^8 m/s).

v = Velocity of propagation of electromagnetic waves through the material comprising the track (e.g., sleeper, ballast, subgrade, etc.)

Measuring the time interval between the reflection of GPR signal from the top and bottom of the characterized layer, such as ballast layer according to Fig. 6, the layer thickness of the media is calculated via:

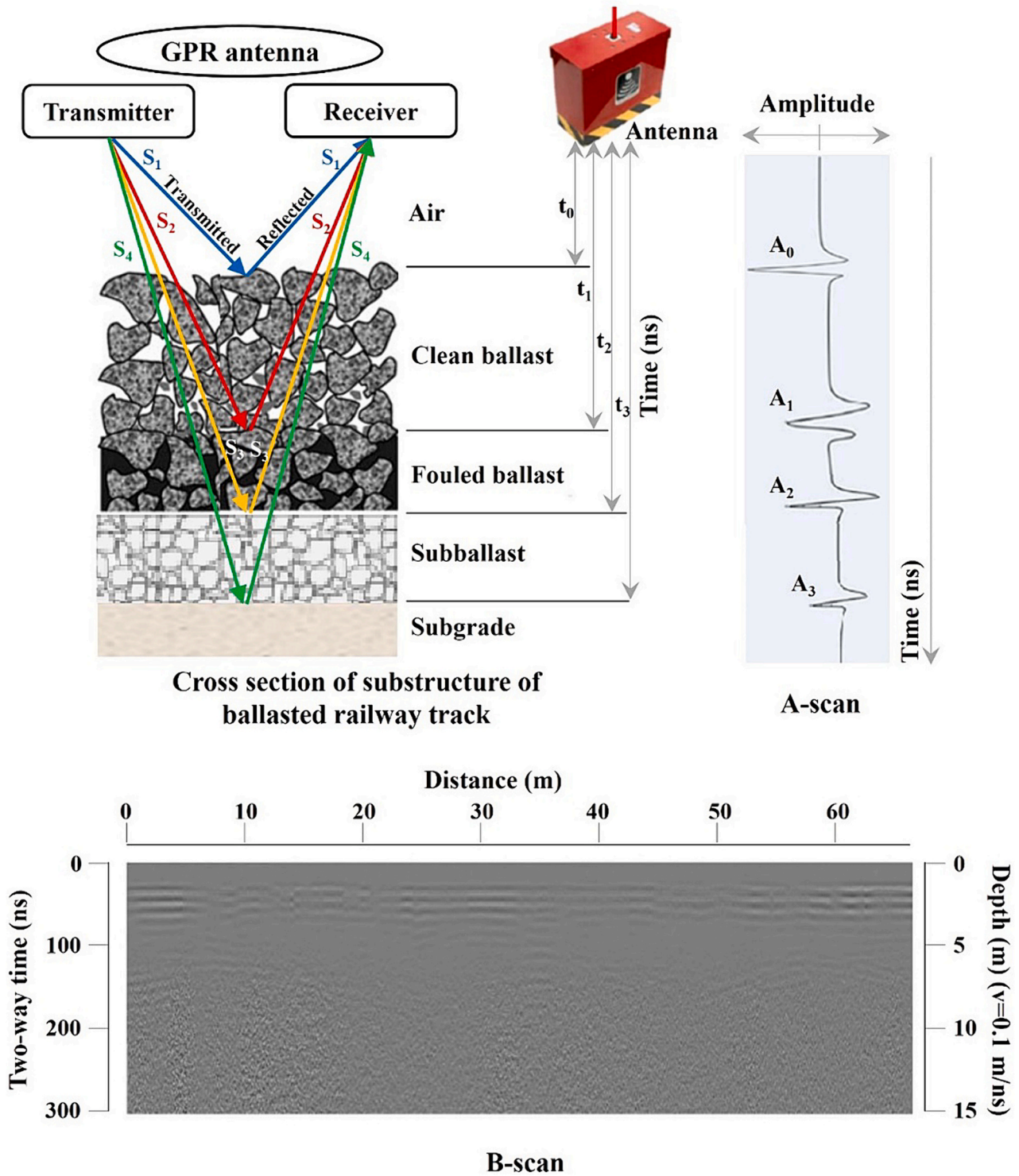


Fig. 6. Main working features of GPR tool for health monitoring of substructure of the railway ballasted tracks [adapted from Ferrante et al. [49], Wang et al. [77], Rasol [78]].

$$h = \frac{v \cdot TWT}{2} \tag{4}$$

h = Thickness of characterized layer.
 TWT = Two-way travel time of the GPR signal.
 when the value of ϵ_r is known, the thickness of characterized layer, such as ballast layer, can be obtained by incorporation of Eq. (3) in Eq. (4):

$$h = \frac{c \cdot TWT}{2\sqrt{\epsilon_r}} \tag{5}$$

Particularly, fouling materials change the dielectric permittivity of ballast layer, based on which GPR data can be used to evaluate ballast layer fouling level. For example, Benedetto et al. [58] mixed clean ballast with different percentages of soil as fouling (0%–24%), and at these fouling percentages, the dielectric permittivity values measured

were between 3.51 and 5.35.

3. InSAR and GPR for infrastructure health monitoring

3.1. Satellite imagery

- Using InSAR to monitor infrastructures

InSAR is recognized as an effective tool for monitoring roadway infrastructures, such as bridge settlements, roadway surface deformations, geohazards, sinkhole detection, historical analysis of problematic sites, as well as determining deformation velocities with millimetric accuracy (see Table 2.a). Fiorentini et al. [79] explored the potential of using SAR-based data to evaluate the quality of road pavements, characterized in terms of the International Roughness Index (IRI). Significant

correlations were observed between IRI values (mm/m) and InSAR estimates (mm/year), though some weak correlations were attributed to local factors, such as pavement materials.

Regarding satellite in airport runway monitoring, Gagliardi et al. [80] compared the capabilities of C-band data acquired by the Sentinel-1 mission to the X-band SAR images obtained from the COSMO-SkyMed mission to gauge the displacements of a runway. The results affirmed the feasibility of using multi-frequency SAR data, especially in pavement management systems, to determine critical displacements and streamline maintenance interventions. As described by Macchiarulo et al. [81], the multi-temporal interferometric synthetic aperture radar (MT-InSAR) technique can measure building displacements over time with millimetre-scale precision, presenting an economical monitoring tool. This method was also employed to assess the damage level of 858 buildings situated near the alignment of twin tunnels.

Table 2

Overview of InSAR application to infrastructure health monitoring: emphasis on railway infrastructures.

a Other civil structures			
Reference	Application	Data acquisition	Target/Conclusion
Fiorentini et al. [79]	<ul style="list-style-type: none"> • Roadway pavement, Milan, Italy 	<ul style="list-style-type: none"> • Sentinel-1 - Using a stack of 210 SAR images (2014–2019) 	<ul style="list-style-type: none"> • Conducting 10-km laser profilometric survey to compute IRI - Correlation between IRI and PS-InSAR data
Karimzadeh and Matsuoka [67]	<ul style="list-style-type: none"> • Land subsidence and pavement monitoring, Tabriz, Iran 	<ul style="list-style-type: none"> • Using X-band COSMO-SkyMed datasets (2017–2018) - Employing SBAS InSAR 	<ul style="list-style-type: none"> • Estimating the land areas affected by land subsidence along with the total length of pavement influenced by subsidence
Macchiarulo et al. [81]	<ul style="list-style-type: none"> • Los Angeles highway and freeway network • Italian motorway network 	<ul style="list-style-type: none"> • Using Sentinel-1 (2016–2019) • Using COSMO-SkyMed datasets (2008–2014) 	<ul style="list-style-type: none"> • Extracting displacement field and deformation velocities from city to national scale
Gagliardi et al. [72]	<ul style="list-style-type: none"> • Rochester Bridge (river bridge), U.K. 	<ul style="list-style-type: none"> • COSMO-SkyMed, X-band (2017–2019) – Employing PS-InSAR 	<ul style="list-style-type: none"> • Health monitoring the structural deformations - Detecting cyclic down-lifting and up-lifting displacements pertinent to seasonal behavior
Gagliardi et al. [80,83]	<ul style="list-style-type: none"> • Airport runway, Rome, Italy 	<ul style="list-style-type: none"> • Sentinel-1 A, C-band (2017–2019) - COSMO-SkyMed, X-band (2017–2019) 	<ul style="list-style-type: none"> • Comparing the results of data processed with the two resolutions – Applying geostatistical analysis
Wu et al. [84]	<ul style="list-style-type: none"> • International airport, Hong Kong 	<ul style="list-style-type: none"> • Using Envisat ASAR, Sentinel-1A, COSMO-SkyMed datasets (1998–2018) - Employing MT-InSAR 	<ul style="list-style-type: none"> • Generating long deformation history
Macchiarulo et al. [85]	<ul style="list-style-type: none"> • Buildings located adjacent to twin tunnels excavations, U.K. 	<ul style="list-style-type: none"> • COSMO-SkyMed MT-InSAR data (2011–2015) 	<ul style="list-style-type: none"> • Evaluation of settlement-induced damage
Jia et al. [70]	<ul style="list-style-type: none"> • Land subsidence along high-speed railway, China 	<ul style="list-style-type: none"> • Landsat images (2014–2018), DEM data - Employing D-InSAR and SBAS-InSAR 	<ul style="list-style-type: none"> • Analyzing the relationship between groundwater flow and land subsidence
Ren et al. [86]	<ul style="list-style-type: none"> • Landslide, China 	<ul style="list-style-type: none"> • Sentinel-1A (2019–2021) - Using ascending-descending orbits and employing SBAS-InSAR 	<ul style="list-style-type: none"> • Identification of potential landslide occurrence by cluster extraction from TS-InSAR analysis and statistical tools
Pedretti et al. [82]	<ul style="list-style-type: none"> • Slow-moving landslide, Italy 	<ul style="list-style-type: none"> • Sentinel-1A (2014–2018), Sentinel-1B (2016–2020) 	<ul style="list-style-type: none"> • Classification of time-series trends to extract active deformations
b Railway infrastructures			
Reference	Application	Data acquisition	Target/Conclusion
Chang et al. [87]	<ul style="list-style-type: none"> • Double track freight railway, Netherlands 	<ul style="list-style-type: none"> • TerraSAR-X (2009–2013) - Employing PS-InSAR 	<ul style="list-style-type: none"> • Estimating displacement time series in both lateral and normal direction (deformation vector) - Detecting vertical displacements due to settlement or compaction - Identifying sudden changes in displacement in transition zone - Needing to control deformation due to placement of track over soft peat and clay soils
Chang et al. [88]	<ul style="list-style-type: none"> • Railway lines, Netherlands 	<ul style="list-style-type: none"> • Radarsat-2 SAR images and 90-m resolution DEM 	<ul style="list-style-type: none"> • Establishing InSAR for monitoring railway infrastructures over nationwide
Poreh et al. [65]	<ul style="list-style-type: none"> • Railway stability, Italy 	<ul style="list-style-type: none"> • Cosmo-SkyMed-X band (2011–2015) 	<ul style="list-style-type: none"> • Detection of possible deformations on the railways - Complying bridge deformations with periodical thermal alterations - Derivation of larger number of PSs by higher resolution imagery
Wang et al. [89]	<ul style="list-style-type: none"> • Railway tracks located on steel bridge and embankment (Transition zone), Netherlands 	<ul style="list-style-type: none"> • TerraSAR-X (2009–2015) • InSAR and data measured by coach and DIC-based device 	<ul style="list-style-type: none"> • Structural health monitoring of transition zones in railway track - Using InSAR system to monitor the health condition of the transition zones between the measurement interval of measuring coaches (half-year) to provide guidance
Chen et al. [90]	<ul style="list-style-type: none"> • Beijing-Tianjin High Speed Railway (BTIR), China 	<ul style="list-style-type: none"> • Envisat ASAR (30-m resolution) (2003–2010), TerraSAR-X (3-m resolution), (2010–2015) - Using SBAS InSAR method 	<ul style="list-style-type: none"> • Evaluating land subsidence along high-speed track
Wang et al. [91]	<ul style="list-style-type: none"> • Beijing-Tianjin Intercity Railway (BTIR), China - Applied for high-speed track 	<ul style="list-style-type: none"> • TerraSAR-X SpotLight images (descending), TerraSAR-X StripMap images (ascending), Sentinel-1 (2015–2017) - Employing PS-InSAR 	<ul style="list-style-type: none"> • Investigating the influence of ground subsidence on the high-speed railway lines – Enriching detailed deformation by establishment of high spatial resolution of TerraSAR-X – Figuring out differential deformation between two tracks of the double-track railway
Shami et al. [92]	<ul style="list-style-type: none"> • Land subsidence along railway track, Iran 	<ul style="list-style-type: none"> • Sentinel-1 (2015–2021) - Using both ascending and descending images 	<ul style="list-style-type: none"> • Assessing ground displacement in the vertical and east-west directions

Considering the use of InSAR for tracking land subsidence and landslides, Jia et al. [70] examined land subsidence along linear engineering areas, like railway lines, employing combined D-InSAR and SBAS-InSAR techniques. They detected five non-uniform settlements, primarily linked to groundwater over-extraction and coal mining. Pedretti et al. [82] used InSAR imagery-based data to monitor slow-moving landslides and instabilities, emphasizing time series (TS) of interferometric satellite data. Regarding continuous observation over the catchment area, it proves beneficial in identifying new active deformations by observing TS trend variations and juxtaposing TS breaks with in-situ monitoring devices. Considering predetermined ground motions, continuously updated satellite data can verify advancing deformations in the studied area and pinpoint new accelerations.

- Using InSAR to monitor railway infrastructures

Given the advantages of SAR interferometry, this technique offers significant support for ground-based methods in monitoring ground deformations around railway tracks, as illustrated in Table 2.b. Chang et al. [88] employed the InSAR time series on nationwide railway networks to produce deformation maps and categorize temporal behavior. This satellite-based survey pinpointed several track segments with pronounced subsidence, especially in areas where the railway was situated on peat soils. Wang et al. [89] contrasted InSAR measurements with data from a measuring coach and a digital image correlation device. The information gathered from InSAR confirmed an intensification in the fluctuation of track alignment near the bridge, representing the transition zone. While SAR satellites offer frequent measurements, the accuracy of these satellite measurements is at the millimetre level, which is relatively modest. Moreover, the spatial resolution/sampling of these measurements is at the meter level, which is broader than the measuring coach's resolution, specifically 0.25 m [89]. Shami et al. [92] harnessed Sentinel-1 data, introducing an innovative method centred on defining a new small baseline subset (NSBAS) to gauge ground subsidence along a railway track situated in central Iran. Their findings indicated that 60% of the railway lines had been impacted by land subsidence.

3.2. Using GPR in railway tracks

GPR is recognized as a well-established NDT technique for monitoring the health of railway track infrastructures (See Table 3). In this context, Al-Qadi et al. [93] identified a strong correlation between

geometric irregularities and the fouling level, quantified through scattering analysis of GPR data. Similarly, other studies have also utilized GPR to assess the condition of fouled ballast layer [94,95]. Bianchini Ciampoli et al. [60] employed GPR on a 30 m-long railway line segment, reproducing various conditions of fragmentation and fouling of ballast. Results of electromagnetic testing affirmed significant effect of fouling on dielectric permittivity of the ballast layer, while also lower influence of fragmentation on this parameter. As noted by Guo et al. [96], the fouling level estimated using GPR deviated by approximately 1–7% compared to traditional sieving results. Similarly, Guo et al. [97] determined indicators based on GPR that aligned well with the fouling index, underscoring the appropriateness of this non-destructive method for simultaneous assessment of railway track conditions.

One of the primary advantages of GPR over InSAR is its ability to assess and predict underlying defects. For example, it can detect ballast fouling in areas with high precipitation and humidity levels, especially when mud pumping occurs on the railway track [98]. Indeed, while GPR is highly beneficial, the integration of supplementary tests and geospatial visualization assessments is essential. This approach underscores the growing focus on combining GPR with imagery-based techniques to enhance the health monitoring of railway ballasted tracks.

Table 4
Main limitations of singular InSAR/GPR application.

InSAR	GPR
1. Availability of permanent scatters or persistent scatters (PS)	1. Limitations on applications for network level/Limited land coverage
2. Unable to identify the conditions of subsurface and sources leading to deteriorations	2. Remarkable time required to investigate the entire transport network
3. Having constraints on spatial resolution/Limitation on data resolution	3. Suppression of signals when passing through the boundary of subsurface layers with heterogeneous conditions
4. Needing big datasets with remarkable size	4. Establishment of advanced processing techniques and experienced surveyor with expert knowledge
	5. Direct effects of material and frequency of antenna on depth of penetration
	6. Iron interference due to special structural components, such as rail guards, steel sleepers, etc.

Table 3
Overview of GPR application to infrastructure health monitoring: emphasis on railway infrastructures.

Reference	Application	Data acquisition	Target/Conclusion
Tosti et al. [99]	<ul style="list-style-type: none"> Laboratory test with a ballast box 	<ul style="list-style-type: none"> GPR with different frequencies spanning from 600 MHz to 2000 MHz 	<ul style="list-style-type: none"> Determining the dielectric permittivity of air-ballast - Following an experimental framework
Bianchini Ciampoli et al. [60]	<ul style="list-style-type: none"> 30-m long railway track, Rome, Italy 	<ul style="list-style-type: none"> GPR with central frequencies of 1000 MHz and 2000 MHz for antenna 	<ul style="list-style-type: none"> Assessing the health condition of railway track beds - Considering the effects of void fouling and degradation of aggregate
Liu et al. [100]	<ul style="list-style-type: none"> A railway line located in a cold area, China 	<ul style="list-style-type: none"> SIR-20 GPR system with antenna frequency of 100 MHz 	<ul style="list-style-type: none"> Detecting the moisture content of railway subgrade
Artagan and Borecky [43]	<ul style="list-style-type: none"> Conducting laboratory test and field track surveying, Czech Republic 	<ul style="list-style-type: none"> Using air-coupled 2 GHz horn antenna, and ground-coupled TR dual-frequency antenna (400/900 MHz) 	<ul style="list-style-type: none"> Assessing railway granite basalt considering distinct fouling and moisture conditions
Liu et al. [101]	<ul style="list-style-type: none"> Construction of a full-scale ballasted track model with 30 m length - Inspection of three railway lines, China 	<ul style="list-style-type: none"> Three-receiver antennas including ground-coupled antennas with frequencies at 400 MHz and 900 MHz, as well as a 2 GHz air-coupled antenna 	<ul style="list-style-type: none"> Inability of 400 MHz antenna to distinguish the interface of clean-fouled ballast
Guo et al. [96]	<ul style="list-style-type: none"> Railway lines, China 	<ul style="list-style-type: none"> Using two 2 GHz air-coupled and one 400 MHz ground-coupled antenna GPR and digging holes for sampling from shoulders 	<ul style="list-style-type: none"> 1–7% difference between NDT results and destructive method based on sieving
Guo et al. [97]	<ul style="list-style-type: none"> Railway lines, China 	<ul style="list-style-type: none"> GPR with three different antennas; For inspection of ballast shoulders and crib 	<ul style="list-style-type: none"> Correlation between GPR results and fouling index - The best correlation between fouling indices based on 5 and 10 mm with FI reflected by GPR
Li et al. [102]	<ul style="list-style-type: none"> 50-km high-speed railway line, southern China 	<ul style="list-style-type: none"> Using air-coupled 2 GHz air-coupled antenna Using gprMax for performing electromagnetic simulation based on the finite-difference time-domain (FDTD) algorithm 	<ul style="list-style-type: none"> Modelling mechanized ballast cleaning on railway ballast Identifying the fouling level along with the cleaning process efficiency

3.3. Limitations of singular application of InSAR or GPR

Table 4 showcases the primary limitations tied to the singular use of InSAR and GPR techniques. On the whole, integrating these proven methods can amalgamate the benefits of each, allowing for a comprehensive data interpretation and effectively addressing the inherent shortcomings of each individual technique.

4. Fusion of different NDT techniques and characterized health monitoring/maintenance plan

4.1. Background on railway infrastructure

Given the advantages and limitations of various established NDT techniques, there is evident value in adopting a combined approach that fuses different NDTs for railway track health monitoring. Regarding the use of multiple NDTs, Fortunato et al. [103] integrated the findings from GPR, FWD, and plate loading tests to effectively rehabilitate the structure of a track bed, taking into account both technical and economic considerations. Similarly, Sussmann and Thompson [104] merged GPR data with FWD results for the maintenance and rehabilitation of railway tracks. Additionally, the fusion of Multi-Temporal InSAR and LiDAR data was identified as another effective method for monitoring deformations along railway systems [105]. Chang et al. [106] aligned the PS-InSAR with LiDAR points to enhance the geolocation accuracy of Sentinel-1 for evaluating line-infrastructures like railway tracks. Moreover, Elseicy et al. [107] provided insights on the synergistic use of GPR and other NDTs, like LiDAR, profilometer, and deflectometer, to assess road pavement conditions. They found that merging such data with geographic information systems (GIS) platforms could significantly enhance pavement management systems.

Selvakumaran et al. [108] took the Waterloo bridge as a case study to gauge the utility of InSAR data for bridge monitoring and compared it with measurements from reflectors placed at strategic structural points, representing in situ measurements. For a holistic assessment of viaducts and bridges' stability, a multi-tiered monitoring strategy was employed, encompassing on-site inspections, ground-based NDTs, and satellite remote sensing examinations [109]. Table 5.a lists studies that explore the integration of various ground-based NDTs with remote sensing techniques for railway infrastructure health monitoring.

4.2. Fusion of InSAR and GPR data to monitor infrastructure

- Integration of InSAR and GPR to monitor civil infrastructures

Satellite-based images are used to monitor surface decay, while GPR is deployed to ascertain the condition of the substructure. Indeed, GPR, a ground-based NDT, is recognized as an effective method for obtaining high-quality data of underlying layers. In addition, satellite remote sensing techniques like InSAR offer both high temporal frequencies and broad inspection coverage areas [32,110]. Given the advantages and limitations of these specific health monitoring approaches, an integration of InSAR and GPR proves beneficial.

In this context, Alani et al. [111] integrated GPR and InSAR to monitor the health of ancient masonry arch bridges. For the InSAR application, Persistent Scatterer Interferometry (PSI) based on C-band images was employed to track the time series of displacements for continuously coherent points, with prospects of future utilization of the X-band. Regarding GPR, a combined use of low and high-frequency GPR was adopted. InSAR's findings corroborated the cyclical upward and downward displacements that occurred due to soil saturation from hydrological cycles, while the high-frequency GPR pinpointed the structural thickness of the layers. Gagliardi et al. [112] merged the results from MT-InSAR based on high-resolution satellite data (X-band) and multi-frequency GPR to evaluate the health of historic masonry arch bridges in Rome, Italy. Time series deformations of persistent scatterers

Table 5

Overview of infrastructure health monitoring by fusing GPR/InSAR with other NDTs: emphasis on railway infrastructures.

a Fusion of InSAR/GPR and other NDT techniques			
Reference	Combined techniques	Application/Target/Damage detected	
Hu et al. [105]	<ul style="list-style-type: none"> • MT-InSAR + LiDAR 	<ul style="list-style-type: none"> • Using LiDAR to overcome the limitations of InSAR associated with positioning accuracy - Using LiDAR for classification of radar scatters - For railway systems 	
Chang et al. [106]	<ul style="list-style-type: none"> • InSAR + LiDAR 	<ul style="list-style-type: none"> • Establishing a fine classification for land deformation based on persistent scatterers (PS) associated to railway infrastructure 	
Selvakumaran et al. [108]	<ul style="list-style-type: none"> • InSAR + Automated Total Station 	<ul style="list-style-type: none"> • Considering Waterloo bridge as a case study 	
Quinci et al. [109]	<ul style="list-style-type: none"> • Ground-based (Laser scanner) + Structural information + RS (MS-InSAR) into GIS 	<ul style="list-style-type: none"> • Bridges mapping in Lazio region, Italy - A premise for development of BMS at a regional level 	
Goodarzi et al. [115]	<ul style="list-style-type: none"> • GPR + LiDAR 	<ul style="list-style-type: none"> • Using LiDAR for assessing the drainage condition of track - Assessing subsurface condition based on GPR data - considering a track with 209 km length 	
Qiu et al. [116]	<ul style="list-style-type: none"> • InSAR + Global navigation satellite system (GNSS) 	<ul style="list-style-type: none"> • Using high spatio-temporal resolution settlement data provided in time series along high-speed railways 	

b Fusion of InSAR and GPR for health monitoring of civil infrastructures			
Reference	Application	Data acquisition	Target/Conclusion
Alani et al. [111]	<ul style="list-style-type: none"> • Masonry arch bridge, Kent, U. K. 	<ul style="list-style-type: none"> • Sentinel-1A (C-band) (2015–2017), GPR with 200, 600 and 2000 MHz antenna - PSI-InSAR 	<ul style="list-style-type: none"> • Using InSAR for structural displacement due to seasonal variations - Using GPR for exact positioning of structural ties
Gagliardi et al. [112]	<ul style="list-style-type: none"> • Masonry bridge, Rome, Italy 	<ul style="list-style-type: none"> • X-band SAR images, Several frequencies of GPR - MT-InSAR 	<ul style="list-style-type: none"> • Monitoring thermal and structural deformations based on processing persistent scatterers
Bianchini Ciampoli et al. [31], Tosti et al. [113]	<ul style="list-style-type: none"> • 26 km of railway stretch for InSAR, and 9.8 km of railway stretch for GPR, Puglia, Southern Italy 	<ul style="list-style-type: none"> • SAR images from both the Sentinel 1A (2017–2018) and COSMO-SkyMed (2016–2018), GPR with operating frequencies of 1000 MHz and 2000 MHz – PS-InSAR 	<ul style="list-style-type: none"> • Evaluating potential subsidence occurring on a railway track - Potential use of InSAR for detecting spots subjected to deformations/Use of GPR data for to diagnose the cause of decay
D'Amico et al. [71]	<ul style="list-style-type: none"> • 12-km long newly build ballasted track, Italy - Focusing on rail-abutment transition area 	<ul style="list-style-type: none"> • Sentinel-1A (2017–2018), COSMO-SkyMed (2016–2018), GPR with 1000 and 2000 frequencies of antenna - 	<ul style="list-style-type: none"> • Estimating the thicknesses of ballast and subballast based on the GPR data - Observing higher land subsidence at the end sections of

(continued on next page)

Table 5 (continued)

b Fusion of InSAR and GPR for health monitoring of civil infrastructures			
Reference	Application	Data acquisition	Target/Conclusion
Bianchini Ciampoli et al. [114]	<ul style="list-style-type: none"> A traditional railway section, Salerno, Italy 	(Permanent scatterers) PS-InSAR <ul style="list-style-type: none"> GPR with different central frequencies + Two-year MT-InSAR analysis 	abutment wing walls <ul style="list-style-type: none"> Integration of two survey methodologies - Detecting subsections of the railway affected by the high rate of ballast fouling - Identifying the poorly bearing subgrade or fragmentation of aggregates as leading to deterioration of track bed

linked to piers and arches, together with B-scan data from GPR, were consolidated for comprehensive health monitoring.

- Integration of InSAR and GPR: emphasis on railway infrastructures

Infrastructures with line networks, such as railway line tracks and pavements, exhibit significant variability in conditions (weather, geography, natural hazards – floods/earthquake/sand storm, etc.), necessitating the use of integrated NDT techniques. The synergistic application of InSAR-based methods complements the leading ground-based NDT, namely GPR, to forge a comprehensive strategy for monitoring railway tracks.

In this context, these methods were combined to assess a 10-km-long existing railway track situated in southern Italy. A significant improvement in the interpretation of GPR data was noted. This enhancement was linked to InSAR's ability to pinpoint critical areas. Specifically, the initial 300 m of the surveyed railway track revealed a correlation between the subsidence detected by InSAR and the attenuation of the GPR signal at the sub-base/subgrade interface [31,113].

D'Amico et al. [71] utilized InSAR and GPR to monitor transition zones of railway tracks, focusing on transition zones (bridge approach). The study demonstrated that InSAR is able to identify problematic areas at the railway line network level. Additional subsidence was observed at the ends of wing walls (Fig. 7a.1), highlighting the diminished lateral retention effect of the wing walls.

Bianchini Ciampoli et al. [114] applied MT-InSAR in tandem with multi-frequency GPR to detect potential deformations in railway lines. They analysed phase changes between multiple images of the same location and the GPR data. The GPR effectively identified varying levels of ballast fouling, while InSAR processing pinpointed the primary causes of track bed deterioration. Fig. 7 showcases examples of the combined use of InSAR and GPR for railway track assessment.

4.3. Integration of InSAR, GPR and machine learning models

This section offers a comprehensive review of relevant journal articles that focus on the use of machine learning (ML) methods and deep learning algorithms. These methodologies are applied to assess the current conditions and enhance the management of various infrastructures by leveraging InSAR and GPR data. In this context, Fig. 8 depicts a schematic representation of ML/DL models integrated with InSAR/GPR for civil engineering infrastructures. Further details, especially those related to railway tracks, are presented below.

Regarding the integration of GPR and ML techniques, Solla et al. [117] explored the feasibility of employing GPR for infrastructures.

They advocated the use of artificial intelligence (AI) to expedite the data interpretation process. Pioneering this field, Shao et al. [118] applied a support vector machine (SVM) to classify ballast fouling conditions. The data used for training and testing the ML model were sourced from three 2-m long railway track sections, representing clean, 50% clay fouling, and 50% coal fouling conditions.

Addressing issues such as mud pumping, subgrade settlement, ballast fouling, and water abnormalities, Xu et al. [119] utilized a Faster R-CNN framework to enhance the identification accuracy of railway subgrade defects using GPR data. Similarly, Liu et al. [120] introduced a deep learning model called CRNN, which combines convolutional neural network (CNN) and recurrent neural network (RNN), for GPR data processing to identify these specific subgrade defects. Detecting sub-surface issues, like potential buried objects, necessitates the examination and interpretation of thousands of GPR images. Therefore, creating an extensive training dataset for ML models emerges as an appropriate approach for GPR data analysis [121]. Concurrently, the development of GPR-focused ML models can assist in streamlining the decision-making process [122].

Considering the InSAR method and noting that utilizing ML methods alongside remote sensing approaches is beneficial for monitoring shorelines [123], this strategy can also be applied to monitor transport infrastructures like railway tracks. Dumitru and Datcu [124] used SVM to explore selected primitive features of high-resolution SAR data for classification. Fiorentini et al. [125] described the combination of PS-InSAR measurements and GIS analyses with ML algorithms to model and predict surface motion ratios due to environmental factors in terms of mm/year for a specific area. In this regard, the maximum entropy model was utilized to identify factors contributing to land subsidence along the Beijing high-speed railway line. Compressible deposit thickness and groundwater levels were considered as input variables, while time series deformation data derived from Envisat and TerraSAR-X images were used as output [90].

Novellino et al. [126] combined ML and InSAR techniques for slow-moving landslide risk assessment. They used InSAR data and aerial photos to develop ensemble models predicting landslide hazards, with horizontal displacement velocity identified as a key factor. Gagliardi et al. [127] applied MT-InSAR on the Rochester bridge in the UK, using X-band images from COSMO-SkyMed (CSM) for PSI analysis and structural displacement monitoring. Additionally, they employed the k-means clustering algorithm, an unsupervised ML approach, to group individual persistent scatter points based on time-series displacements and deformation patterns. This enhanced the detection of critical areas in transport infrastructure monitoring.

Naghibi et al. [128] combined InSAR and ML to predict ground subsidence rates in arid regions. For ML model development, which included the BRT and XGB algorithms, factors like topography, climate, hydrogeology, and anthropogenic influences were considered as contributors to land subsidence. Mirmazloumi et al. [129] employed various ML models to categorize InSAR-provided big data representing ground motion. This classification aimed to identify trends based on various displacement rates, including stable, linear, bilinear, quadratic, and PUE. Random forest and extreme gradient boosting emerged as the most effective ML models for accurate data labelling. Conversely, CNN and RNN were deemed more suitable for smaller regions considering accuracy and computational time.

Rygu et al. [130] used the Hierarchical Density-Based Spatial Clustering of Applications with Noise (HDBSCAN) ML algorithm to measure the deformation of Indonesia's Bandung Basin. This clustering method helped identify areas with unique acceleration and deceleration deformation patterns.

4.4. Railway track health monitoring and maintenance implementation

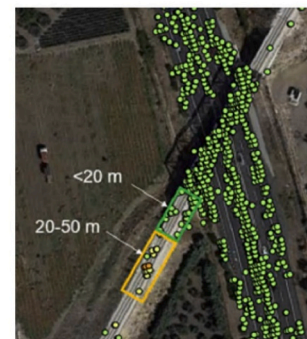
Executing a series of structured tasks is vital to maintain optimal operational conditions of railway tracks and optimize cost-effective



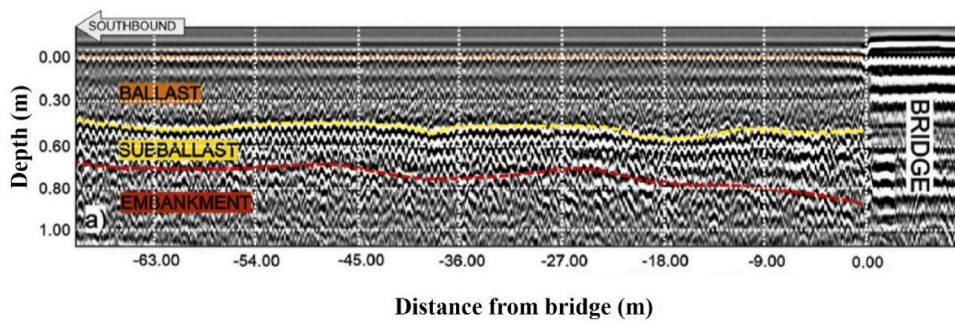
a.1 Wing walls



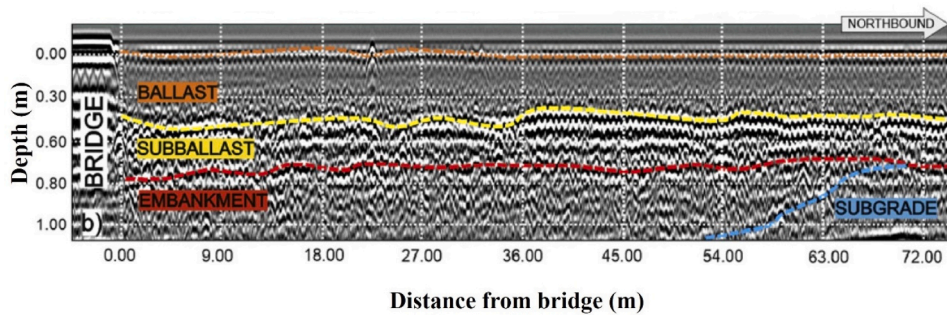
a.2 PS-InSAR analysis of northbound



a.3 PS-InSAR analysis of southbound



a.4 Radargram based on the GPR data collected before the rail truss bridge (Southbound)

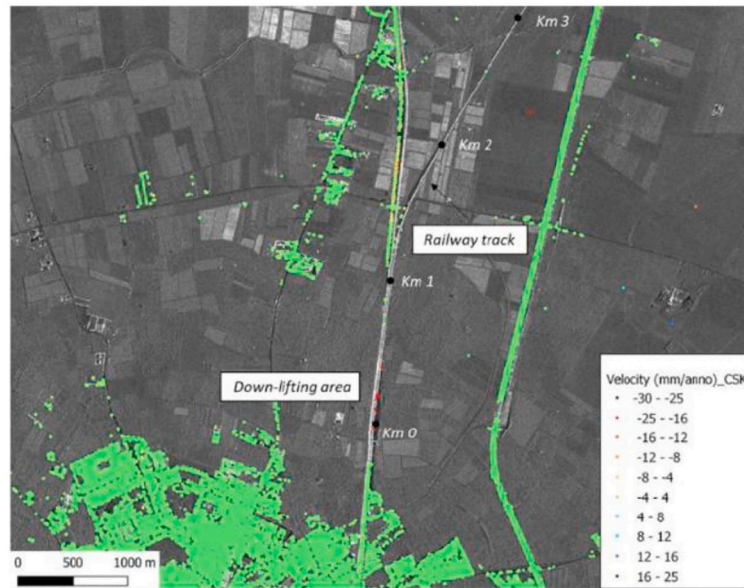


a.5 Radargram based on the GPR data collected after the rail truss bridge (Northbound)

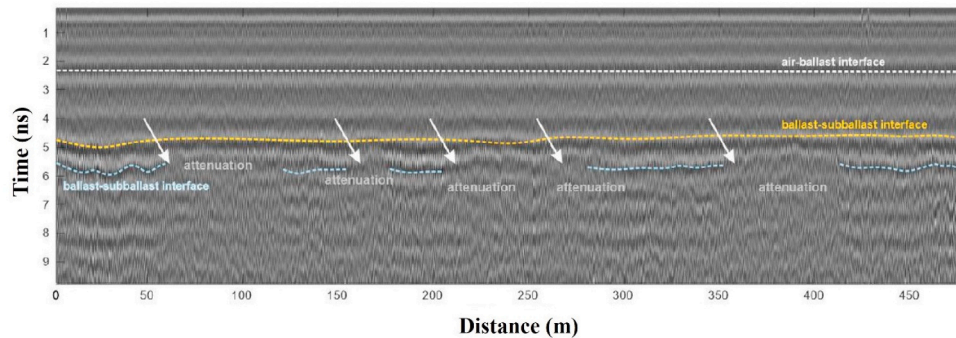
a Subsidence of transitions areas in railway bridges (figure reproduced with permission from [71]

published by Elsevier)

Fig. 7. Examples of fusion of InSAR/GPR techniques for health monitoring of railway tracks, b Analysis of space-born and round-born data for detecting deformation along an existing railway track bed (figure reproduced with permission from [113] published by Elsevier).



b.1 Rate of land subsidence based on the PS-InSAR analysis applied on SAR images



b.2 Radargram based on the GPR data collected at the subsidence spot detected from InSAR analysis

Fig. 7. (continued).

inspection/maintenance intervals. Maintenance plans are traditionally categorized into preventive, corrective, and run-to-failure strategies. As depicted in Fig. 9.a, the preventive strategy comprises subdivisions such as timely-scheduled, condition-based, and predictive approaches.

The combined outputs from InSAR and GPR offer a diagnostic system for defect identification, establishing a condition-based maintenance plan that covers both the railway line scale and network scale. Beyond merging GPR and InSAR datasets, the emergence of ML techniques for classification, clustering, and regression enhances the management of large datasets related to transport infrastructure health monitoring, especially railway tracks. Consequently, a predictive methodology can be formulated using continuous monitoring of railway lines with data from InSAR/GPR, assisting in the development of trained ML/DL models, as illustrated in Fig. 9.b.

Earlier studies [146–148] have suggested that a condition-based approach, rather than a strictly timed program, is more beneficial. For example, Guler [146] enhanced maintenance activities for ballasted railway tracks using genetic algorithms within a condition-based framework. Additionally, Zhang et al. [148] created predictive models from periodic GPS displacement measurements to examine landslide conditions. In terms of predictive track maintenance, Lasisi and Attoh-Okiné [149] considered three significant geometric parameters to build an ML model that classifies track sections as defective or non-defective based on a combined track quality index. Similarly, data-

driven models emphasizing preventive maintenance were expanded, with the track's geometric condition as the dependent variable and standard deviations of longitudinal level and rail alignment as independent variables [150]. Beyond established ML models, Sresakoolchai and Kaewunruen [151] used the proximal policy optimization, a reinforcement learning algorithm, to decrease carbon emissions from railway maintenance activities, considering several track geometry parameters and maintenance actions. This methodology effectively developed predictive maintenance from the available data.

In conclusion, crafting a predictive strategy using imagery data and geometric parameters for railway asset management results in optimal maintenance timings. This not only reduces overall maintenance costs throughout a railway system's life but also prevents disruptions due to unforeseen significant failures. In terms of cost-benefit analysis, SAR-based methodologies are seen more as complementary tools, rather than replacements, for traditional inspection methods, facilitating continuous infrastructure monitoring and early fault detection [152]. Concurrently, the integrated use of InSAR and GPR for continuous railway infrastructure monitoring emphasizes a proactive approach in maintenance planning.

The broad coverage of the InSAR technique, combined with GPR's ability to pinpoint defect origins, aids in developing a comprehensive management system for railway tracks, spanning from railway line to network scales. In this context, Fontul et al. [153] introduced a speedier

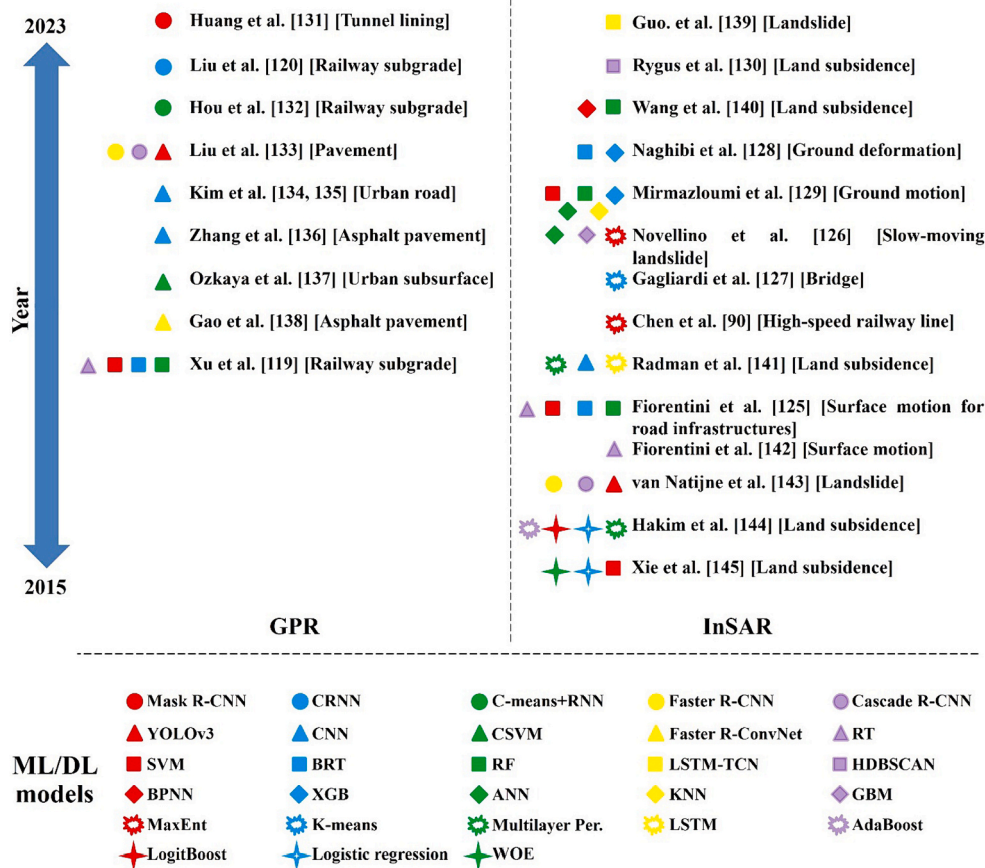


Fig. 8. Illustrative layout of ML models incorporated in InSAR/GPR for civil engineering infrastructures [90,119,120,125–145].

processing method to use GPR at the network level, employing an accelerated frequency domain analysis for surveying extended railway line sections. Ferrante et al. [49] emphasized the importance of expanding NDTs from local to network levels to effectively map railway lines. Considering spatial scales, data from integrated InSAR and GPR can be further processed using GIS, enhancing maintenance planning [154]. Therefore, merging data from SAR and GPR tools can elevate railway infrastructure health monitoring to a network scale, with the application of ML/DL models further enhancing predictive maintenance strategies.

5. Conclusions and perspectives

This paper reviews non-destructive testing techniques applying to civil infrastructure health monitoring. It emphasized on the application of InSAR and GPR fusion to railway track inspection/monitoring, as well as integration of machine learning (or artificial intelligence) into monitoring data processing and prediction, finally reaching the aim of smart railway asset management (emphasis on railway track condition-based maintenance). Based on the review of literature and discussions on the technology feasibility study, the following conclusions are given.

- To address the technological limitations of standalone health monitoring methods, the fusion of InSAR and GPR proves beneficial. The InSAR technique offers a vast coverage area combined with the potential for intermittent data acquisition. Thus, this method is well-suited for elevating established health monitoring to a network level. Concurrently, critical locations identified using the SAR tool can be further investigated with GPR to pinpoint the origins of defects.

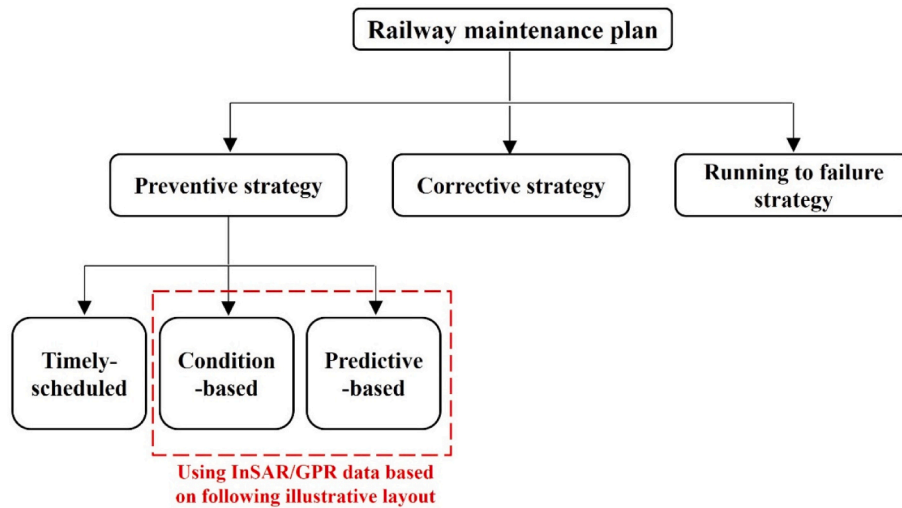
- Continuous measurements along railway tracks using InSAR techniques yield vast amounts of imagery data. These can be processed with ML/DL methods to formulate predictive models based on ground motion trends and displacement classifications. As a result, predictive maintenance strategies become more practical than either timely-scheduled or corrective approaches. This ensures decision-makers have the necessary information to determine optimal inspection and maintenance timings for railway tracks.
- Currently, the integration of InSAR and GPR techniques is still evolving. This highlights the need for further exploration and application of these combined methods for railway infrastructure. Examples include monitoring land subsidence alongside railway tracks, identifying widespread defects, and detecting multiple anomalies. When considering machine learning and deep learning algorithms, a future endeavour involving these integrated techniques should aim to develop this combined process on a network level. This would enable the identification of critical areas based on deformation rates or trend predictions, while also utilizing GPR at the local level for supplementary analyses.

Compliance with ethical standards

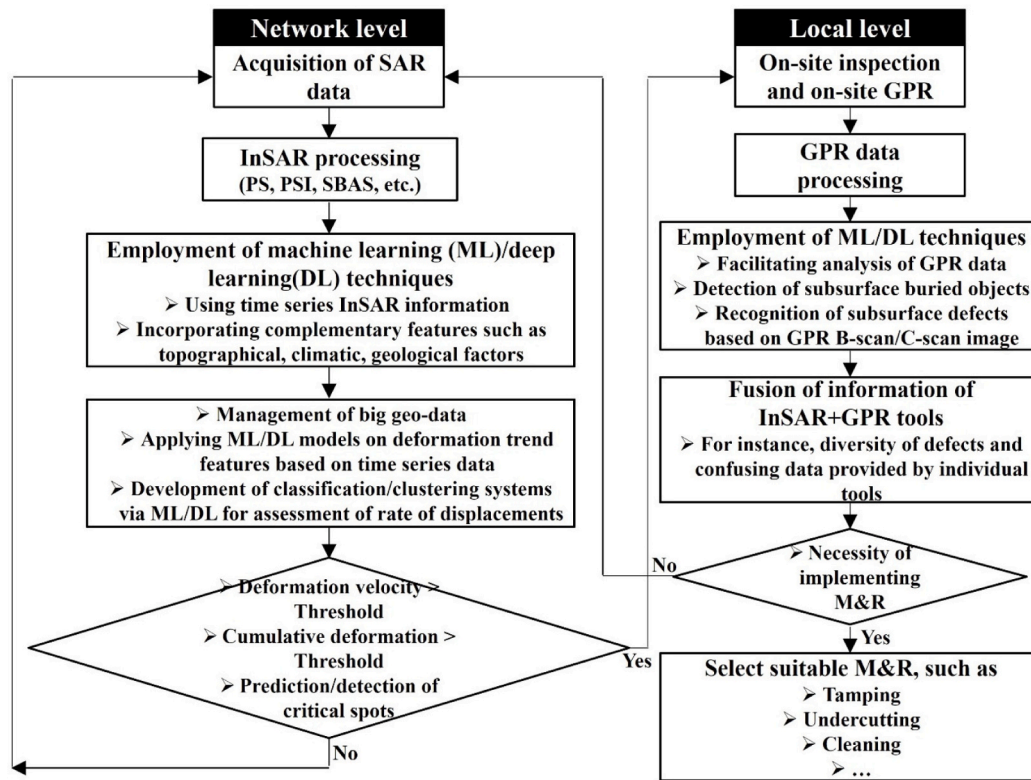
The authors declare that there is no conflict of interest regarding the publication of this article.

CRediT authorship contribution statement

Mehdi Koohmishi: Data curation, Investigation, Resources, Writing – original draft, Writing – review & editing. **Sakdirat Kaewunruen:** Conceptualization, Funding acquisition, Methodology, Supervision, Writing – review & editing. **Ling Chang:** Conceptualization,



9.a Process of management of railway infrastructures considering monitoring and maintenance plans



9.b Process of fusion of InSAR/GPR techniques for health monitoring of railway infrastructures

Fig. 9. Health monitoring and maintenance implementing plan for railway infrastructures: A focus on predictive management based on the fusion of outputs of InSAR and GPR along with employment of ML/DL models [adapted from Gagliardi et al. [32], Ferrante et al. [49]].

Methodology, Resources, Supervision, Validation, Writing – review & editing. **Yunlong Guo:** Conceptualization, Funding acquisition, Investigation, Methodology, Resources, Visualization, Writing – original draft, Writing – review & editing.

Declaration of competing interest

The authors declared that they have no conflicts of interest to this work.

We declare that we do not have any commercial or associative

interest that represents a conflict of interest in connection with the work submitted.

Data availability

Data will be made available on request.

Acknowledgements

The European Commission and UKRI Engineering and Physical

Science Research Council (EPSRC) are acknowledged for the financial sponsorship of Re4Rail project (Grant No EP/Y015401/1).

References

- [1] B. Indraratna, S.S. Nimbalkar, N.T. Ngo, T. Neville, Performance improvement of rail track substructure using artificial inclusions—experimental and numerical studies, *Transp. Geotech.* 8 (2016) 69–85, <https://doi.org/10.1016/j.trgeo.2016.04.001>.
- [2] C.N. Pyrgidis, *Railway Transportation Systems: Design, Construction and Operation*, CRC Press, 2021 (ISBN: 9780367494230).
- [3] E.T. Selig, J.M. Waters, *Track geotechnology and substructure management*. 1994, Thomas Telford, 1994. ISBN: 978-0727720139.
- [4] D. Li, J. Hyslip, T. Sussmann, S. Chrismer, *Railway Geotechnics*, CRC Press, 2015. ISBN: 9780367866594.
- [5] I.L. Al-Qadi, W. Xie, R. Roberts, Z. Leng, Data analysis techniques for GPR used for assessing railroad ballast in high radio-frequency environment, *J. Transp. Eng.* 136 (4) (2010) 392–399, [https://doi.org/10.1061/\(ASCE\)TE.1943-5436.000008](https://doi.org/10.1061/(ASCE)TE.1943-5436.000008).
- [6] K. Tzanakakis, *The Railway Track and its Long Term Behaviour: A Handbook for a Railway Track of High Quality vol. 2*, Springer Science & Business Media, 2013. ISBN: 978-3-642-36050-3.
- [7] S. Jovanovic, H. Guler, B. Coko, Track degradation analysis in the scope of railway infrastructure maintenance management systems, *Gradevinar* 67 (3) (2015) 247–257, <https://doi.org/10.14256/JCE.1194.2014>.
- [8] S. Bressi, J. Santos, M. Losa, Optimization of maintenance strategies for railway track-bed considering probabilistic degradation models and different reliability levels, *Reliab. Eng. Syst. Saf.* 207 (2021) 107359, <https://doi.org/10.1016/j.res.2020.107359>.
- [9] F.K. Rioja, Filling potholes: macroeconomic effects of maintenance versus new investments in public infrastructure, *J. Public Econ.* 87 (9–10) (2003) 2281–2304, [https://doi.org/10.1016/S0047-2727\(01\)00200-6](https://doi.org/10.1016/S0047-2727(01)00200-6).
- [10] W. Zhao, W. Qiang, F. Yang, G. Jing, Y. Guo, Data-driven ballast layer degradation identification and maintenance decision based on track geometry irregularities, *Int. J. Rail Transp.* (2023) 1–23, <https://doi.org/10.1080/23248378.2023.2228802>.
- [11] C. Charoenwong, D.P. Connolly, A. Colaço, P.A. Costa, P.K. Woodward, A. Romero, P. Galvín, Railway slab vs ballasted track: a comparison of track geometry degradation, *Constr. Build. Mater.* 378 (2023) 131121, <https://doi.org/10.1016/j.conbuildmat.2023.131121>.
- [12] C. Shen, P. Zhang, R. Dollevoet, A. Zoeteman, Z. Li, Evaluating railway track stiffness using axle box accelerations: a digital twin approach, *Mech. Syst. Signal Process.* 204 (2023) 110730, <https://doi.org/10.1016/j.ymsp.2023.110730>.
- [13] S.S. Artagan, L. Bianchini Ciampoli, F. D'Amico, A. Calvi, F. Tosti, Non-destructive assessment and health monitoring of railway infrastructures, *Surv. Geophys.* 41 (2020) 447–483, <https://doi.org/10.1007/s10712-019-09544-w>.
- [14] Y. Guo, V. Markine, G. Jing, Review of ballast track tamping: mechanism, challenges and solutions, *Constr. Build. Mater.* 300 (2021) 123940, <https://doi.org/10.1016/j.conbuildmat.2021.123940>.
- [15] J. Zhao, A.H.C. Chan, A.B. Stirling, K.B. Madelin, Optimizing policies of railway ballast tamping and renewal, *Transp. Res. Rec.* 1943 (1) (2006) 50–56, <https://doi.org/10.1177/0361198106194300107>.
- [16] T. Dahlberg, *Railway track settlements—a literature review*, in: Report for the EU project Supertrack 463, 2004.
- [17] Q.D. Sun, B. Indraratna, S. Nimbalkar, Deformation and degradation mechanisms of railway ballast under high frequency cyclic loading, *J. Geotech. Geoenviron. Eng.* 142 (1) (2016) 04015056, [https://doi.org/10.1061/\(ASCE\)GT.1943-5606.0001375](https://doi.org/10.1061/(ASCE)GT.1943-5606.0001375).
- [18] H. Huang, E. Tutumluer, Discrete element modeling for fouled railroad ballast, *Constr. Build. Mater.* 25 (8) (2011) 3306–3312, <https://doi.org/10.1016/j.conbuildmat.2011.03.019>.
- [19] A.K. Rohman, H.F. Kashani, C.L. Ho, Effects of natural abrasion on railroad ballast strength and deformation properties, *Constr. Build. Mater.* 247 (2020) 118315, <https://doi.org/10.1016/j.conbuildmat.2020.118315>.
- [20] M.J. Roshan, A.S.A. Rashid, N.A. Wahab, S. Tamassoki, S.N. Jusoh, M.A. Hezmi, N.N.N. Daud, N.M. Apandi, M. Azmi, Improved methods to prevent railway embankment failure and subgrade degradation: a review, *Transp. Geotech.* 37 (2022) 100834, <https://doi.org/10.1016/j.trgeo.2022.100834>.
- [21] Z. Meng, C. Liyi, W. Shanyong, W. Honggang, Experimental study of the microstructure of loess on its macroscopic geotechnical properties of the Baozhong railway subgrade in Ningxia, China, *Bull. Eng. Geol. Environ.* 79 (2020) 4829–4840, <https://doi.org/10.1007/s10064-020-01816-9>.
- [22] J. Liu, J. Xiao, Experimental study on the stability of railroad silt subgrade with increasing train speed, *J. Geotech. Geoenviron. Eng.* 136 (6) (2010) 833–841, [https://doi.org/10.1061/\(ASCE\)GT.1943-5606.0000282](https://doi.org/10.1061/(ASCE)GT.1943-5606.0000282).
- [23] I. Lee, Y.T. Choi, M. Lee, C.Y. Yune, Effect of groundwater level variation on residual settlement of Korean high-speed railway on soft ground, *KSCE J. Civ. Eng.* 22 (2018) 3312–3320, <https://doi.org/10.1007/s12205-017-0472-6>.
- [24] J. Sadeghi, H. Askarinejad, An investigation into the effects of track structural conditions on railway track geometry deviations, *Proc. Inst. Mech. Eng. Part F J. Rail Rapid Transit* 223 (4) (2009) 415–425, <https://doi.org/10.1243/09544097JRR266>.
- [25] O. Nabochenko, M. Sysyn, V. Kovalchuk, Y. Kovalchuk, A. Pensak, S. Braichenko, Studying the railroad track geometry deterioration as a result of an uneven subsidence of the ballast layer, *Eastern-Eur. J. Enterp. Technol.* 97 (7) (2019), <https://doi.org/10.15587/1729-4061.2019.154864>.
- [26] X. Wang, X. Liu, T.L. Euston, Relationship between track geometry defect occurrence and substructure condition: a case study on one passenger railroad in the United States, *Constr. Build. Mater.* 365 (2023) 130066, <https://doi.org/10.1016/j.conbuildmat.2022.130066>.
- [27] M. Macchi, M. Garetti, D. Centrone, L. Fumagalli, G.P. Pavirani, Maintenance management of railway infrastructures based on reliability analysis, *Reliab. Eng. Syst. Saf.* 104 (2012) 71–83, <https://doi.org/10.1016/j.res.2012.03.017>.
- [28] M. Burkhalter, B.T. Adey, Digitalizing the determination of railway infrastructure intervention programs: a network optimization model, *J. Infrastruct. Syst.* 28 (2) (2022) 04022012, [https://doi.org/10.1061/\(ASCE\)IS.1943-555X.0000681](https://doi.org/10.1061/(ASCE)IS.1943-555X.0000681).
- [29] G. Bureika, G. Vaiciunas, D. Shi, A.C. Zanuy, Influence of track geometry condition monitoring on railway infrastructure maintenance processing, *Transp. Probl.* 17 (4) (2022) 211–220, <https://doi.org/10.20858/tp.2022.17.4.18>.
- [30] S. Wang, G. Liu, G. Jing, Q. Feng, H. Liu, Y. Guo, State-of-the-art review of ground penetrating radar (GPR) applications for railway ballast inspection, *Sensors* 22 (7) (2022) 2450, <https://doi.org/10.3390/s22072450>.
- [31] L. Bianchini Ciampoli, V. Gagliardi, C. Clementini, D. Latini, F. Del Frate, A. Benedetto, Transport infrastructure monitoring by InSAR and GPR data fusion, *Surv. Geophys.* 41 (2020) 371–394, <https://doi.org/10.1007/s10712-019-09563-7>.
- [32] V. Gagliardi, F. Tosti, L. Bianchini Ciampoli, M.L. Battagliere, L. D'Amato, A. M. Alani, A. Benedetto, Satellite remote sensing and non-destructive testing methods for transport infrastructure monitoring: advances, challenges and perspectives, *Remote Sens.* 15 (2) (2023) 418, <https://doi.org/10.3390/rs15020418>.
- [33] V. Gagliardi, L. Bianchini Ciampoli, S. Trevisani, F. D'Amico, A.M. Alani, A. Benedetto, F. Tosti, Testing Sentinel-1 SAR interferometry data for airport runway monitoring: a geostatistical analysis, *Sensors* 21 (17) (2021) 5769, <https://doi.org/10.3390/s21175769>.
- [34] F. Tosti, A. Benedetto, L. Bianchini Ciampoli, F. D'Amico, C. Plati, A. Loizos, Guest editorial: data fusion, integration and advances of non-destructive testing methods in civil and environmental engineering, *NDT & E Int.* (2020), <https://doi.org/10.1016/j.ndteint.2020.102286>.
- [35] P.M. Atkinson, Downscaling in remote sensing, *Int. J. Appl. Earth Obs. Geoinf.* 22 (2013) 106–114, <https://doi.org/10.1016/j.jag.2012.04.012>.
- [36] F. D'Amico, L. Bertolini, A. Napolitano, D.R.J. Manalo, V. Gagliardi, L. B. Ciampoli, Implementation of an interoperable BIM platform integrating ground-based and remote sensing information for network-level infrastructures monitoring, in: *Earth Resources and Environmental Remote Sensing/GIS Applications XIII Vol. 12268*, SPIE, 2022, pp. 112–122, <https://doi.org/10.1117/12.2638108>.
- [37] L. Bertolini, F. D'Amico, A. Napolitano, L. Bianchini Ciampoli, V. Gagliardi, Romer Diezmas Manalo, J., A BIM-based approach for pavement monitoring integrating data from non-destructive testing methods (NDTs), *Infrastructures* 8 (5) (2023) 81, <https://doi.org/10.3390/infrastructures8050081>.
- [38] Available online, www.scopus.com (accessed on 30 January 2024).
- [39] M. Moaveni, Y. Qian, I.I. Qamhia, E. Tutumluer, C. Basye, D. Li, Morphological characterization of railroad ballast degradation trends in the field and laboratory, *Transp. Res. Rec.* 2545 (1) (2016) 89–99, <https://doi.org/10.3141/2545-10>.
- [40] F.M.C.P. Fernandes, M. Pereira, A.G. Correia, L. Caldeira, P.B. Lourenço, Assessment of layer thickness and uniformity in railway embankments with ground penetrating radar, 2008. ISBN: 9780415475907.
- [41] Z. Leng, I.L. Al-Qadi, Railroad ballast evaluation using ground-penetrating radar: laboratory investigation and field validation, *Transp. Res. Rec.* 2159 (1) (2010) 110–117, <https://doi.org/10.3141/2159-14>.
- [42] H.F. Kashani, C.L. Ho, W.P. Clement, C.P. Oden, Evaluating the correlation between the geotechnical index and the electromagnetic properties of fouled ballasted track by a full-scale laboratory model, *Transp. Res. Rec.* 2545 (1) (2016) 66–78, <https://doi.org/10.3141/2545-08>.
- [43] S.S. Artagan, V. Borecky, Advances in the nondestructive condition assessment of railway ballast: a focus on GPR, *NDT & E Int.* 115 (2020) 102290, <https://doi.org/10.1016/j.ndteint.2020.102290>.
- [44] D. Mishra, E. Tutumluer, T.D. Stark, J.P. Hyslip, S.M. Chrismer, M. Tomas, Investigation of differential movement at railroad bridge approaches through geotechnical instrumentation, *J. Zhejiang Univ. Sci. A* 13 (2012) 814–824, <https://doi.org/10.1631/jzus.A12ISG7>.
- [45] D. Mishra, E. Tutumluer, H. Boler, J.P. Hyslip, T.R. Sussmann, Railroad track transitions with multidepth deflectometers and strain gauges, *Transp. Res. Rec.* 2448 (1) (2014) 105–114, <https://doi.org/10.3141/2448-13>.
- [46] Y. Haddani, P. Breul, G. Saussine, M.A.B. Navarrete, F. Ranvier, R. Gourvès, Trackbed mechanical and physical characterization using PANDA®/geoenoscopy coupling, *Procedia Eng.* 143 (2016) 1201–1209, <https://doi.org/10.1016/j.proeng.2016.06.118>.
- [47] J.R. Vivanco, S. Barbier, M.A.B. Navarrete, P. Breul, Statistical analysis of the influence of ballast fouling on penetrometer and geoenoscopy data, in: *Advances in Transportation Geotechnics IV: Proceedings of the 4th International Conference on Transportation Geotechnics Volume 2*, Springer International Publishing, Cham, 2021, pp. 915–930, https://doi.org/10.1007/978-3-030-77234-5_75.
- [48] M. Papaelias, C. Roberts, C.L. Davis, A review on non-destructive evaluation of rails: state-of-the-art and future development, *Proc. Inst. Mech. Eng. Part F J. Rail and Rapid Transit* 222 (4) (2008) 367–384, <https://doi.org/10.1243/09544097JRR209>.

- [49] C. Ferrante, L. Bianchini Ciampoli, A. Benedetto, A.M. Alani, F. Tosti, Non-destructive technologies for sustainable assessment and monitoring of railway infrastructure: a focus on GPR and InSAR methods, *Environ. Earth Sci.* 80 (24) (2021) 806, <https://doi.org/10.1007/s12665-021-10068-z>.
- [50] G. Liu, J. Cong, P. Wang, S. Du, L. Wang, R. Chen, Study on vertical vibration and transmission characteristics of railway ballast using impact hammer test, *Constr. Build. Mater.* 316 (2022) 125898, <https://doi.org/10.1016/j.conbuildmat.2021.125898>.
- [51] P. Haji Abdulrazzag, O. Farzaneh, C. Behnia, Evaluation of railway trackbed moduli using the rail falling weight test method and its backcalculation model, *Proc. Inst. Mech. Eng. Part F J. Rail Rapid Transit* 233 (4) (2019) 431–447, <https://doi.org/10.1177/0954409718799800>.
- [52] M. Moaveni, S. Wang, J.M. Hart, E. Tutumluer, N. Ahuja, Evaluation of aggregate size and shape by means of segmentation techniques and aggregate image processing algorithms, *Transp. Res. Rec.* 2335 (1) (2013) 50–59, <https://doi.org/10.3141/2335-06>.
- [53] H. Huang, M. Moaveni, S. Schmidt, E. Tutumluer, J.M. Hart, Evaluation of railway ballast permeability using machine vision-based degradation analysis, *Transp. Res. Rec.* 2672 (10) (2018) 62–73, <https://doi.org/10.1177/0361198118790849>.
- [54] S. Schmidt, S. Shah, M. Moaveni, B.J. Landry, E. Tutumluer, C. Basye, D. Li, Railway ballast permeability and cleaning considerations, *Transp. Res. Rec.* 2607 (1) (2017) 24–32, <https://doi.org/10.3141/2607-05>.
- [55] M. Guerrieri, G. Parla, C. Celauro, Digital image analysis technique for measuring railway track defects and ballast gradation, *Measurement* 113 (2018) 137–147, <https://doi.org/10.1016/j.measurement.2017.08.040>.
- [56] S.K. Hussaini, B. Indraratna, J.S. Vinod, Application of optical-fiber Bragg grating sensors in monitoring the rail track deformations, *Geotech. Test. J.* 38 (4) (2015) 387–396, <https://doi.org/10.1520/GTJ20140123>.
- [57] D. Sasi, S. Philip, R. David, J. Swathi, A review on structural health monitoring of railroad track structures using fiber optic sensors, *Mater. Today Proc.* 33 (2020) 3787–3793, <https://doi.org/10.1016/j.matpr.2020.06.217>.
- [58] A. Benedetto, F. Tosti, L.B. Ciampoli, A. Calvi, M.G. Brancadoro, A.M. Alani, Railway ballast condition assessment using ground-penetrating radar—An experimental, numerical simulation and modelling development, *Constr. Build. Mater.* 140 (2017) 508–520, <https://doi.org/10.1016/j.conbuildmat.2017.02.110>.
- [59] L. Bianchini Ciampoli, A. Calvi, F. D'Amico, Railway ballast monitoring by GPR: a test-site investigation, *Remote Sens.* 11 (20) (2019) 2381, <https://doi.org/10.3390/rs11202381>.
- [60] L. Bianchini Ciampoli, A. Calvi, E. Oliva, Test-site operations for the health monitoring of railway ballast using ground-penetrating radar, *Transp. Res. Procedia* 45 (2020) 763–770, <https://doi.org/10.1016/j.trpro.2020.02.099>.
- [61] E. Aldao, H. González-Jorge, L.M. González-deSantos, G. Fontenla-Carrera, J. Martínez-Sánchez, Validation of solid-state lidar measurement system for ballast geometry monitoring in rail tracks, *Infrastructures* 8 (4) (2023) 63, <https://doi.org/10.3390/infrastructures8040063>.
- [62] X. Liang, X. Niu, P. Liu, C. Lan, R. Yang, Z. Zhou, Test on fouling detection of ballast based on infrared thermography, *NDT & E Int.* 140 (2023) 102956, <https://doi.org/10.1016/j.ndteint.2023.102956>.
- [63] Y. Narazaki, V. Hoskere, G. Chowdhary, B.F. Spencer Jr., Vision-based navigation planning for autonomous post-earthquake inspection of reinforced concrete railway viaducts using unmanned aerial vehicles, *Autom. Constr.* 137 (2022) 104214, <https://doi.org/10.1016/j.autcon.2022.104214>.
- [64] A.K. Singh, A. Swarup, A. Agarwal, D. Singh, Vision based rail track extraction and monitoring through drone imagery, *ICT Express* 5 (4) (2019) 250–255, <https://doi.org/10.1016/j.icte.2017.11.010>.
- [65] D. Poreh, A. Iodice, D. Riccio, G. Ruello, Railways' stability observed in Campania (Italy) by InSAR data, *Eur. J. Remote Sens.* 49 (1) (2016) 417–431, <https://doi.org/10.5721/EurJRS20164923>.
- [66] Y. Wassie, Q. Gao, O. Monserrat, A. Barra, B. Crippa, M. Crosetto, Differential SAR interferometry for the monitoring of land subsidence along railway infrastructures, *Int. Arch. Photogramm. Remote. Sens. Spat. Inf. Sci.* 43 (2022) 361–366, <https://doi.org/10.5194/isprs-archives-XLIII-B3-2022-361-2022>.
- [67] S. Karimzadeh, M. Matsuoka, Remote sensing X-band SAR data for land subsidence and pavement monitoring, *Sensors* 20 (17) (2020) 4751, <https://doi.org/10.3390/s20174751>.
- [68] M.Z.I. Bashar, *Leveraging Satellite Data and Machine Learning to Enhance Pavement Condition Assessment*, Doctoral dissertation, University of Colorado at Boulder, 2022.
- [69] A. Ferretti, C. Prati, F. Rocca, Nonlinear subsidence rate estimation using permanent scatterers in differential SAR interferometry, *IEEE Trans. Geosci. Remote Sens.* 38 (5) (2000) 2202–2212, <https://doi.org/10.1109/36.868878>.
- [70] C. Jia, X. Yang, J. Wu, P. Ding, C. Bian, Monitoring analysis and numerical simulation of the land subsidence in linear engineering areas, *KSCIE J. Civ. Eng.* 25 (7) (2021) 2674–2689, <https://doi.org/10.1007/s12205-021-1823-x>.
- [71] F. D'Amico, V. Gagliardi, L.B. Ciampoli, F. Tosti, Integration of InSAR and GPR techniques for monitoring transition areas in railway bridges, *NDT & E Int.* 115 (2020) 102291, <https://doi.org/10.1016/j.ndteint.2020.102291>.
- [72] V. Gagliardi, L. Bianchini Ciampoli, F. D'Amico, A.M. Alani, F. Tosti, A. Benedetto, Multi-temporal SAR interferometry for structural assessment of bridges: the rochester bridge case study, in: *Airfield and Highway Pavements 2021*, 2021, pp. 308–319. ISBN: 9780784483527.
- [73] R. Lanari, F. Casu, M. Manzo, G. Zeni, P. Berardino, M. Manunta, A. Pepe, An overview of the small baseline subset algorithm: A DInSAR technique for surface deformation analysis, in: *Deformation and Gravity Change: Indicators of Isostasy, Tectonics, Volcanism, and Climate Change*, 2007, pp. 637–661, https://doi.org/10.1007/978-3-7643-8417-3_2.
- [74] M. Crosetto, O. Monserrat, M. Cuevas-González, N. Devanthery, B. Crippa, Persistent scatterer interferometry: a review, *ISPRS J. Photogramm. Remote Sens.* 115 (2016) 78–89, <https://doi.org/10.1016/j.isprsjprs.2015.10.011>.
- [75] T.R. Sussmann, E.T. Selig, J.P. Hyslip, Railway track condition indicators from ground penetrating radar, *NDT Int.* 36 (3) (2003) 157–167, [https://doi.org/10.1016/S0963-8695\(02\)00054-3](https://doi.org/10.1016/S0963-8695(02)00054-3).
- [76] R. Roberts, I. Al-Audi, E. Tutumluer, J. Boyle, Subsurface evaluation of railway track using ground penetrating radar, Federal Railroad Administration, 2008. Available: <https://railroads.dot.gov/elibrary/subsurface-evaluation-railway-track-using-groundpenetrating-radar>.
- [77] H. Wang, M. Silvast, V. Markine, B. Wiljanen, Analysis of the dynamic wheel loads in railway transition zones considering the moisture condition of the ballast and subballast, *Appl. Sci.* 7 (12) (2017) 1208, <https://doi.org/10.3390/app7121208>.
- [78] M.A.R. Rasol, *Development of New GPR Methodologies for Soil and Concrete Pavement Assessment*, Polytechnic University of Catalonia (UPC), Barcelona, Spain, 2021, <https://doi.org/10.5821/dissertation-2117-345315>.
- [79] N. Fiorentini, M. Maboudi, P. Leandri, M. Losa, Can machine learning and PS-InSAR reliably stand in for road profilometric surveys? *Sensors* 21 (10) (2021) 3377, <https://doi.org/10.3390/s21103377>.
- [80] V. Gagliardi, L.B. Ciampoli, F. D'Amico, A.M. Alani, F. Tosti, M.L. Battagliere, A. Benedetto, Novel perspectives in the monitoring of transport infrastructures by Sentinel-1 and COSMO-SkyMed Multi-Temporal SAR Interferometry, in: *2021 IEEE International Geoscience and Remote Sensing Symposium IGARSS, IEEE, 2021, July, pp. 1891–1894*, <https://doi.org/10.1109/IGARSS47720.2021.9553749>.
- [81] V. Macchiarulo, P. Milillo, M.J. DeJong, J. Gonzalez Marti, J. Sánchez, G. Giardina, Integrated InSAR monitoring and structural assessment of tunnelling-induced building deformations, *Struct. Control. Health Monit.* 28 (9) (2021) e2781, <https://doi.org/10.1002/stc.2781>.
- [82] L. Pedretti, M. Bordini, V. Vivaldi, S. Fignini, M. Parnigoni, A. Grossi, L. Lanteri, M. Tararbra, N. Negro, C. Meisina, Interpolation of InSAR time series for the detection of ground deformation events (ONtheMOVE): application to slow-moving landslides, *Landslides* (2023) 1–17, <https://doi.org/10.1007/s10346-023-02073-z>.
- [83] V. Gagliardi, L. Bianchini Ciampoli, S. Trevisani, F. D'Amico, A.M. Alani, A. Benedetto, F. Tosti, Testing Sentinel-1 SAR interferometry data for airport runway monitoring: a geostatistical analysis, *Sensors* 21 (17) (2021) 5769, <https://doi.org/10.3390/s21175769>.
- [84] S. Wu, Z. Yang, X. Ding, B. Zhang, L. Zhang, Z. Lu, Two decades of settlement of Hong Kong international airport measured with multi-temporal InSAR, *Remote Sens. Environ.* 248 (2020) 111976, <https://doi.org/10.1016/j.rse.2020.111976>.
- [85] V. Macchiarulo, P. Milillo, C. Blenkinsopp, G. Giardina, Monitoring deformations of infrastructure networks: a fully automated GIS integration and analysis of InSAR time-series, *Struct. Health Monit.* 21 (4) (2022) 1849–1878, <https://doi.org/10.1177/14759217211045912>.
- [86] T. Ren, W. Gong, L. Gao, F. Zhao, Z. Cheng, An interpretation approach of ascending-descending SAR data for landslide identification, *Remote Sens.* 14 (5) (2022) 1299, <https://doi.org/10.3390/rs14051299>.
- [87] L. Chang, R.P.B.J. Dollevoet, R.F. Hanssen, Railway infrastructure monitoring using satellite radar data, *Int. J. Railway Technol.* 3 (2014) 79–91, <https://doi.org/10.4203/ijrt.3.2.5>.
- [88] L. Chang, R.P. Dollevoet, R.F. Hanssen, Nationwide railway monitoring using satellite SAR interferometry, *IEEE J. Sel. Top. Appl. Earth Obs. Remote Sens.* 10 (2) (2016) 596–604, <https://doi.org/10.1109/JSTARS.2016.2584783>.
- [89] H. Wang, L. Chang, V. Markine, Structural health monitoring of railway transition zones using satellite radar data, *Sensors* 18 (2) (2018) 413, <https://doi.org/10.3390/s18020413>.
- [90] B. Chen, H. Gong, Y. Chen, K. Lei, C. Zhou, Y. Si, X. Li, Y. Pan, M. Gao, Investigating land subsidence and its causes along Beijing high-speed railway using multi-platform InSAR and a maximum entropy model, *Int. J. Appl. Earth Obs. Geoinf.* 96 (2021) 102284, <https://doi.org/10.1016/j.jag.2020.102284>.
- [91] Y. Wang, Z. Bai, Y. Zhang, Y. Qin, Y. Lin, Y. Li, W. Shen, Using TerraSAR X-band and sentinel-1 C-band SAR interferometry for deformation along Beijing-Tianjin intercity railway analysis, *IEEE J. Sel. Top. Appl. Earth Obs. Remote Sens.* 14 (2021) 4832–4841, <https://doi.org/10.1109/JSTARS.2021.3076244>.
- [92] S. Shami, M.K. Azar, F. Nilfouroushan, M. Salimi, M.A.M. Reshadi, Assessments of ground subsidence along the railway in the Kashan plain, Iran, using Sentinel-1 data and NSBAS algorithm, *Int. J. Appl. Earth Obs. Geoinf.* 112 (2022) 102898, <https://doi.org/10.1016/j.jag.2022.102898>.
- [93] I.L. Al-Qadi, W. Xie, R. Roberts, Scattering analysis of ground-penetrating radar data to quantify railroad ballast contamination, *NDT & E Int.* 41 (6) (2008) 441–447, <https://doi.org/10.1016/j.ndteint.2008.03.004>.
- [94] P. Shangguan, I.L. Al-Qadi, Z. Leng, Ground-penetrating radar data to develop wavelet technique for quantifying railroad ballast-fouling conditions, *Transp. Res. Rec.* 2289 (1) (2012) 95–102, <https://doi.org/10.3141/2289-13>.
- [95] P. Anbazhagan, P.N. Dixit, T.P. Bharatha, Identification of type and degree of railway ballast fouling using ground coupled GPR antennas, *J. Appl. Geophys.* 126 (2016) 183–190, <https://doi.org/10.1016/j.jappgeo.2016.01.018>.
- [96] Y. Guo, S. Wang, G. Jing, F. Yang, G. Liu, W. Qiang, Y. Wang, Assessment of ballast layer under multiple field conditions in China, *Constr. Build. Mater.* 340 (2022) 127740, <https://doi.org/10.1016/j.conbuildmat.2022.127740>.

- [97] Y. Guo, G. Liu, G. Jing, J. Qu, S. Wang, W. Qiang, Ballast fouling inspection and quantification with ground penetrating radar (GPR), *Int. J. Rail Transp.* 11 (2) (2023) 151–168, <https://doi.org/10.1080/23248378.2022.2064346>.
- [98] C. Kuo, C. Hsu, Y. Chen, C. Wu, H. Wang, D. Chen, Y. Lin, Using ground-penetrating radar to promote the investigating efficiency in mud pumping disaster of railways, *Proc. Eng. Technol. Innov.* 4 (2016) 49–51. Available, <http://ojs.imeiti.org/index.php/PETI/article/view/257>.
- [99] F. Tosti, A. Benedetto, A. Calvi, L.B. Ciampoli, Laboratory investigations for the electromagnetic characterization of railway ballast through GPR, in: 2016 16th International Conference on Ground Penetrating Radar (GPR), IEEE, 2016, June, pp. 1–6, <https://doi.org/10.1109/ICGPR.2016.7572605>.
- [100] S. Liu, Q. Lu, H. Li, Y. Wang, Estimation of moisture content in railway subgrade by ground penetrating radar, *Remote Sens.* 12 (18) (2020) 2912, <https://doi.org/10.3390/rs12182912>.
- [101] G. Liu, Z. Peng, G. Jing, S. Wang, Y. Li, Y. Guo, Railway ballast layer inspection with different GPR antennas and frequencies, *Transp. Geotech.* 36 (2022) 100823, <https://doi.org/10.1016/j.trgeo.2022.100823>.
- [102] B. Li, Z. Peng, S. Wang, L. Guo, Identification of ballast fouling status and mechanized cleaning efficiency using FDTD method, *Remote Sens.* 15 (13) (2023) 3437, <https://doi.org/10.3390/rs15133437>.
- [103] E. Fortunato, S. Fontul, A. Paixão, N. Cruz, J. Cruz, F. Asseseiro, *Geotechnical aspects of the rehabilitation of a freight railway line in Africa*, in: Proceedings of the Third International Conference on Railway Technology: Research, Development and Maintenance in Cagliari, Sardinia, Italy, Civil-Comp Press, Stirlingshire, 2016. ISBN: 9781905088652.
- [104] T.R. Sussmann, H.B. Thompson, Track structural design for maintenance and rehabilitation with automated track inspection data, in: 11th International Heavy Haul Association. South Africa, Cape Town, 2017.
- [105] F. Hu, F.J.V. Leijen, L. Chang, J. Wu, R.F. Hanssen, Monitoring deformation along railway systems combining multi-temporal InSAR and LiDAR data, *Remote Sens.* 11 (19) (2019) 2298, <https://doi.org/10.3390/rs11192298>.
- [106] L. Chang, N.P. Sakpal, S.O. Elberink, H. Wang, Railway infrastructure classification and instability identification using Sentinel-1 SAR and laser scanning data, *Sensors* 20 (24) (2020) 7108, <https://doi.org/10.3390/s20247108>.
- [107] A. Elseicy, A. Alonso-Díaz, M. Solla, M. Rasol, S. Santos-Assunção, Combined use of GPR and other NDTs for road pavement assessment: An overview, *Remote Sens.* 14 (17) (2022) 4336, <https://doi.org/10.3390/rs14174336>.
- [108] S. Selvakumaran, C. Rossi, A. Marinoni, G. Webb, J. Bennetts, E. Barton, S. Plank, C. Middleton, Combined InSAR and terrestrial structural monitoring of bridges, *IEEE Trans. Geosci. Remote Sens.* 58 (10) (2020) 7141–7153, <https://doi.org/10.1109/TGRS.2020.2979961>.
- [109] G. Quinci, V. Gagliardi, L. Pallante, D.R.J. Manalo, A. Napolitano, L. Bertolini, L. B. Ciampoli, P. Meriggi, F. D'Amico, F. Paolacci, A novel bridge monitoring system implementing ground-based, structural and remote sensing information into a GIS-based catalogue, in: Earth Resources and Environmental Remote Sensing/GIS Applications XIII vol. 12268, SPIE, 2022, October, pp. 101–111, <https://doi.org/10.1117/12.2637913>.
- [110] F. Tosti, V. Gagliardi, L.B. Ciampoli, A. Benedetto, S. Threader, A.M. Alani, Integration of remote sensing and ground-based non-destructive methods in transport infrastructure monitoring: Advances, challenges and perspectives, in: 2021 IEEE Asia-Pacific Conference on Geoscience, Electronics and Remote Sensing Technology (AGERS), IEEE, 2021, September, pp. 1–7, <https://doi.org/10.1109/AGERS53903.2021.9617280>.
- [111] A.M. Alani, F. Tosti, L.B. Ciampoli, V. Gagliardi, A. Benedetto, An integrated investigative approach in health monitoring of masonry arch bridges using GPR and InSAR technologies, *NDT & E Int.* 115 (2020) 102288, <https://doi.org/10.1016/j.ndteint.2020.102288>.
- [112] V. Gagliardi, L.B. Ciampoli, F. D'Amico, A. Benedetto, Integrated health monitoring of masonry arch bridges by remote sensing and ground penetrating radar technologies, in: Earth Resources and Environmental Remote Sensing/GIS Applications XIII vol. 12268, SPIE, 2022, October, pp. 72–81, <https://doi.org/10.1117/12.2638935>.
- [113] F. Tosti, V. Gagliardi, F. D'Amico, A.M. Alani, Transport infrastructure monitoring by data fusion of GPR and SAR imagery information, *Transp. Res. Procedia* 45 (2020) 771–778, <https://doi.org/10.1016/j.trpro.2020.02.097>.
- [114] L. Bianchini Ciampoli, V. Gagliardi, F. D'Amico, C. Clementini, D. Latini, A. Benedetto, Quality Assessment in Railway Ballast by Integration of NDT Methods and Remote Sensing Techniques: A Study Case in Salerno, Southern Italy (No. EGU22-2712). Copernicus Meetings, 2022, <https://doi.org/10.5194/egusphere-egu22-2712>.
- [115] S. Goodarzi, H.F. Kashani, A. Saedi, J. Oke, C.L. Ho, Stochastic analysis for estimating track geometry degradation rates based on GPR and LiDAR data, *Constr. Build. Mater.* 369 (2023) 130591, <https://doi.org/10.1016/j.conbuildmat.2023.130591>.
- [116] D. Qiu, Y. Wang, Y. Zhang, Y. Tong, H. Liang, K.L. Ding, S. Wan, J. Wang, Settlement monitoring data fusion approach for high-speed railways based on GNSS and InSAR, *J. Appl. Remote. Sens.* 17 (3) (2023) 034507, <https://doi.org/10.1117/1.JRS.17.034507>.
- [117] M. Solla, V. Pérez-Gracia, S. Fontul, A review of GPR application on transport infrastructures: troubleshooting and best practices, *Remote Sens.* 13 (4) (2021) 672, <https://doi.org/10.3390/rs13040672>.
- [118] W. Shao, A. Bouzerdoum, S.L. Phung, L. Su, B. Indraratna, C. Rujikiatkamjorn, Automatic classification of ground-penetrating-radar signals for railway-ballast assessment, *IEEE Trans. Geosci. Remote Sens.* 49 (10) (2011) 3961–3972, <https://doi.org/10.1109/TGRS.2011.2128328>.
- [119] X. Xu, Y. Lei, F. Yang, Railway subgrade defect automatic recognition method based on improved faster R-CNN, *Sci. Program.* 2018 (2018), <https://doi.org/10.1155/2018/4832972>.
- [120] H. Liu, S. Wang, G. Jing, Z. Yu, J. Yang, Y. Zhang, Y. Guo, Combined CNN and RNN neural networks for GPR detection of railway subgrade diseases, *Sensors* 23 (12) (2023) 5383, <https://doi.org/10.3390/s23125383>.
- [121] M. Boldt, A. Thiele, K. Schulz, Training data generation for machine learning using GPR images, in: Earth Resources and Environmental Remote Sensing/GIS Applications XIII vol. 12268, SPIE, 2022, October, pp. 82–88, <https://doi.org/10.1117/12.2635714>.
- [122] M. Rasol, J.C. Pais, V. Pérez-Gracia, M. Solla, F.M. Fernandes, S. Fontul, D. Ayala-Cabrera, F. Schmidt, H. Assadollahi, GPR monitoring for road transport infrastructure: a systematic review and machine learning insights, *Constr. Build. Mater.* 324 (2022) 126686, <https://doi.org/10.1016/j.conbuildmat.2022.126686>.
- [123] C.A.D. Tsiakos, C. Chalkias, Use of machine learning and remote sensing techniques for shoreline monitoring: a review of recent literature, *Appl. Sci.* 13 (5) (2023) 3268, <https://doi.org/10.3390/app13053268>.
- [124] C.O. Dumitru, M. Datcu, Information content of very high resolution SAR images: study of feature extraction and imaging parameters, *IEEE Trans. Geosci. Remote Sens.* 51 (8) (2013) 4591–4610, <https://doi.org/10.1109/TGRS.2013.2265413>.
- [125] N. Fiorentini, M. Maboudi, P. Leandri, M. Losa, M. Gerke, Surface motion prediction and mapping for road infrastructures management by PS-InSAR measurements and machine learning algorithms, *Remote Sens.* 12 (23) (2020) 3976, <https://doi.org/10.3390/rs12233976>.
- [126] A. Novellino, M. Cesarano, P. Cappelletti, D. Di Martire, M. Di Napoli, M. Ramondini, A. Sowter, D. Calcaterra, Slow-moving landslide risk assessment combining machine learning and InSAR techniques, *Catena* 203 (2021) 105317, <https://doi.org/10.1016/j.catena.2021.105317>.
- [127] V. Gagliardi, F. Tosti, L.B. Ciampoli, F. D'Amico, A.M. Alani, M.L. Battagliere, A. Benedetto, Monitoring of bridges by MT-InSAR and unsupervised machine learning clustering techniques, in: Earth Resources and Environmental Remote Sensing/GIS Applications XII vol. 11863, SPIE, 2021, September, pp. 132–140, <https://doi.org/10.1117/12.2597509>.
- [128] S.A. Naghibi, B. Khodaei, H. Hashemi, An integrated InSAR-machine learning approach for ground deformation rate modeling in arid areas, *J. Hydrol.* 608 (2022) 127627, <https://doi.org/10.1016/j.jhydrol.2022.127627>.
- [129] S.M. Mirmazloumi, A.F. Gambin, R. Palamà, M. Crosetto, Y. Wassie, J.A. Navarro, A. Barra, O. Monserrat, Supervised machine learning algorithms for ground motion time series classification from InSAR data, *Remote Sens.* 14 (15) (2022) 3821, <https://doi.org/10.3390/rs14153821>.
- [130] M. Rygus, A. Novellino, E. Hussain, F. Syafudin, H. Andreas, C. Meisina, A clustering approach for the analysis of InSAR time series: application to the Bandung Basin (Indonesia), *Remote Sens.* 15 (15) (2023) 3776, <https://doi.org/10.3390/rs15153776>.
- [131] J. Huang, X. Yang, F. Zhou, X. Li, B. Zhou, S. Lu, S. Ivashov, I. Giannakis, F. Kong, E. Slob, A deep learning framework based on improved self-supervised learning for ground-penetrating radar tunnel lining inspection, *Comput. Aid. Civ. Inf. Eng.* (2023), <https://doi.org/10.1111/mice.13042>.
- [132] Z. Hou, W. Zhao, Y. Yang, Identification of railway subgrade defects based on ground penetrating radar, *Sci. Rep.* 13 (1) (2023) 6030, <https://doi.org/10.1038/s41598-023-33278-w>.
- [133] Z. Liu, X. Gu, W. Wu, X. Zou, Q. Dong, L. Wang, GPR-based detection of internal cracks in asphalt pavement: a combination method of DeepAugment data and object detection, *Measurement* 197 (2022) 111281, <https://doi.org/10.1016/j.measurement.2022.111281>.
- [134] N. Kim, K. Kim, Y.K. An, H.J. Lee, J.J. Lee, Deep learning-based underground object detection for urban road pavement, *Int. J. Pavement Eng.* 21 (13) (2020) 1638–1650, <https://doi.org/10.1080/10298436.2018.1559317>.
- [135] N. Kim, S. Kim, Y.K. An, J.J. Lee, A novel 3D GPR image arrangement for deep learning-based underground object classification, *Int. J. Pavement Eng.* 22 (6) (2021) 740–751, <https://doi.org/10.1080/10298436.2019.1645846>.
- [136] J. Zhang, X. Yang, W. Li, S. Zhang, Y. Jia, Automatic detection of moisture damages in asphalt pavements from GPR data with deep CNN and IRS method, *Autom. Constr.* 113 (2020) 103119, <https://doi.org/10.1016/j.autcon.2020.103119>.
- [137] U. Ozkaya, F. Melgani, M.B. Bejiga, L. Seyfi, M. Donelli, GPR B scan image analysis with deep learning methods, *Measurement* 165 (2020) 107770, <https://doi.org/10.1016/j.measurement.2020.107770>.
- [138] J. Gao, D. Yuan, Z. Tong, J. Yang, D. Yu, Autonomous pavement distress detection using ground penetrating radar and region-based deep learning, *Measurement* 164 (2020) 108077, <https://doi.org/10.1016/j.measurement.2020.108077>.
- [139] H. Guo, Y. Yuan, J. Wang, J. Cui, D. Zhang, R. Zhang, Q. Cao, J. Li, W. Dai, H. Bao, B. Qiao, Large-scale land subsidence monitoring and prediction based on SBAS-InSAR technology with time-series sentinel-1A satellite data, *Remote Sens.* 15 (11) (2023) 2843, <https://doi.org/10.3390/rs15112843>.
- [140] H. Wang, C. Jia, P. Ding, K. Feng, X. Yang, X. Zhu, Analysis and prediction of regional land subsidence with InSAR technology and machine learning algorithm, *KSCE J. Civ. Eng.* 27 (2) (2023) 782–793, <https://doi.org/10.1007/s12205-022-1067-4>.
- [141] A. Radman, M. Akhoondzadeh, B. Hosseiny, Integrating InSAR and deep-learning for modeling and predicting subsidence over the adjacent area of Lake Urmia, Iran, *GISci. Remote Sens.* 58 (8) (2021) 1413–1433, <https://doi.org/10.1080/15481603.2021.1991689>.
- [142] N. Fiorentini, M. Maboudi, M. Losa, M. Gerke, Assessing resilience of infrastructures towards exogenous events by using ps-insar-based surface motion

- estimates and machine learning regression techniques, *ISPRS Ann. Photogram. Remote Sens. Spat. Inform. Sci.* 4 (2020) 19–26, <https://doi.org/10.5194/isprs-annals-V-4-2020-19-2020>.
- [143] A.L. van Natiijne, R.C. Lindenbergh, T.A. Bogaard, Machine learning: new potential for local and regional deep-seated landslide nowcasting, *Sensors* 20 (5) (2020) 1425, <https://doi.org/10.3390/s20051425>.
- [144] W.L. Hakim, A.R. Achmad, C.W. Lee, Land subsidence susceptibility mapping in Jakarta using functional and meta-ensemble machine learning algorithm based on time-series InSAR data, *Remote Sens.* 12 (21) (2020) 3627, <https://doi.org/10.3390/rs12213627>.
- [145] Z. Xie, G. Chen, X. Meng, Y. Zhang, L. Qiao, L. Tan, A comparative study of landslide susceptibility mapping using weight of evidence, logistic regression and support vector machine and evaluated by SBAS-InSAR monitoring: Zhouqu to Wudu segment in Bailong River Basin, China, *Environ. Earth Sci.* 76 (2017) 1–19, <https://doi.org/10.1007/s12665-017-6640-7>.
- [146] H. Guler, Optimisation of railway track maintenance and renewal works by genetic algorithms, *Gradevinar* 68 (12) (2016) 979–993, <https://doi.org/10.14256/JCE.1458.2015>.
- [147] T. Dong, R.T. Haftka, N.H. Kim, Advantages of condition-based maintenance over scheduled maintenance using structural health monitoring system, in: *Reliability and Maintenance - An Overview of Cases*, 2019, <https://doi.org/10.5772/intechopen.83614>.
- [148] Y.G. Zhang, J. Tang, Z.Y. He, J. Tan, C. Li, A novel displacement prediction method using gated recurrent unit model with time series analysis in the Erdaohe landslide, *Nat. Hazards* 105 (2021) 783–813, <https://doi.org/10.1007/s11069-020-04337-6>.
- [149] A. Lasisi, N. Attoh-Okine, Principal components analysis and track quality index: a machine learning approach, *Transp. Res. Part C Emerg. Technol.* 91 (2018) 230–248, <https://doi.org/10.1016/j.trc.2018.04.001>.
- [150] C. Vale, M.L. Simões, Prediction of railway track condition for preventive maintenance by using a data-driven approach, *Infrastructures* 7 (3) (2022) 34, <https://doi.org/10.3390/infrastructures7030034>.
- [151] J. Sresakoolchai, S. Kaewunruen, Interactive reinforcement learning innovation to reduce carbon emissions in railway infrastructure maintenance, *Dev. Built Environ.* 15 (2023) 100193, <https://doi.org/10.1016/j.dibe.2023.100193>.
- [152] A. Ozden, A. Faghri, M. Li, K. Tabrizi, Evaluation of synthetic aperture radar satellite remote sensing for pavement and infrastructure monitoring, *Procedia Eng.* 145 (2016) 752–759, <https://doi.org/10.1016/j.proeng.2016.04.098>.
- [153] S. Fontul, A. Paixão, M. Solla, L. Pajewski, Railway track condition assessment at network level by frequency domain analysis of GPR data, *Remote Sens.* 10 (4) (2018) 559, <https://doi.org/10.3390/rs10040559>.
- [154] F. Orellana, P.J. D'Aranno, S. Scifoni, M. Marsella, SAR interferometry data exploitation for infrastructure monitoring using GIS application, *Infrastructures* 8 (5) (2023) 94, <https://doi.org/10.3390/infrastructures8050094>.